**Table 2** In-hospital mortality of hepatectomy, RFA, and TAE

| | Hepatectomy | | | RFA | | | TAE | | |
|---|---|---|---|---|---|---|---|---|---|
| | *n/N* | % (95 % CI) | *P* | *n/N* | % (95 % CI) | *P* | *n/N* | % (95 % CI) | *P* |
| Overall | 137/5,270 | 2.60 (2.19–3.10) | | 29/11,688 | 0.25 (0.17–0.36) | | 383/37,187 | 1.03 (0.93–1.14) | |
| Sex | | | 0.26 | | | 0.08 | | | 0.17 |
| Female | 38/1,250 | 3.04 (2.16–4.15) | | 14/3,831 | 0.37 (0.20–0.61) | | 93/10,185 | 0.91 (0.73–1.12) | |
| Male | 99/4,020 | 2.46 (2.01–3.00) | | 15/7,857 | 0.19 (0.11–0.31) | | 290/27,002 | 1.07 (0.95–1.20) | |
| Age (years) | | | 0.002 | | | 0.001 | | | 0.04 |
| ≤59 | 10/883 | 1.13 (0.54–2.07) | | 0/1,197 | 0.0 (0.00–0.30) | | 45/3,418 | 1.32 (0.96–1.76) | |
| 60–69 | 40/1,703 | 2.35 (1.68–3.18) | | 2/3,162 | 0.06 (0.01–0.23) | | 112/9,797 | 1.14 (0.94–1.37) | |
| 70–79 | 76/2,261 | 3.36 (2.66–4.19) | | 19/5,471 | 0.35 (0.21–0.54) | | 163/17,515 | 0.93 (0.79–1.08) | |
| ≥80 | 11/423 | 2.60 (1.31–4.61) | | 8/1,858 | 0.43 (0.19–0.85) | | 63/6,457 | 0.98 (0.75–1.25) | |
| Procedure type | | | <0.001 | | | | | | |
| Partial hepatectomy | 42/2,163 | 1.94 (1.40–2.62) | | – | | | – | | |
| Segmentectomy | 45/1,921 | 2.34 (1.71–3.12) | | – | | | – | | |
| Lobectomy | 31/869 | 3.57 (2.44–5.03) | | – | | | – | | |
| Extended lobectomy | 19/317 | 6.00 (3.65–9.20) | | – | | | – | | |
| Hospital volume[a] | | | <0.001 | | | 0.26 | | | <0.001 |
| High | 27/1,744 | 1.55 (1.02–2.24) | | 8/3,875 | 0.21 (0.09–0.41) | | 97/12,101 | 0.80 (0.65–0.98) | |
| Intermediate | 38/1,742 | 2.18 (1.55–3.00) | | 8/3,896 | 0.21 (0.09–0.40) | | 126/12,497 | 1.01 (0.84–1.20) | |
| Low | 72/1,784 | 4.04 (3.17–5.06) | | 13/3,917 | 0.33 (0.18–0.57) | | 160/12,589 | 1.27 (1.08–1.48) | |
| Comorbidities | | | | | | | | | |
| Diabetes mellitus | | | 0.97 | | | 0.68 | | | 0.76 |
| No | 107/4,108 | 2.60 (2.14–3.14) | | 25/9,743 | 0.26 (0.17–0.38) | | 311/30,416 | 1.02 (0.91–1.14) | |
| Yes | 30/1,162 | 2.58 (1.75–3.67) | | 4/1,945 | 0.21 (0.06–0.53) | | 72/6,771 | 1.06 (0.83–1.34) | |
| Cardiac diseases | | | 0.93 | | | <0.001 | | | 0.79 |
| No | 129/4,953 | 2.60 (2.18–3.09) | | 24/11,323 | 0.21 (0.14–0.32) | | 369/35,731 | 1.03 (0.93–1.14) | |
| Yes | 8/317 | 2.52 (1.10–4.91) | | 5/365 | 1.37 (0.45–3.17) | | 14/1,456 | 0.96 (0.53–1.61) | |
| Chronic renal diseases | | | 0.02 | | | 0.52 | | | 0.29 |
| No | 132/5,198 | 2.54 (2.13–3.00) | | 29/11,527 | 0.25 (0.17–0.36) | | 375/36,649 | 1.02 (0.92–1.13) | |
| Yes | 5/72 | 6.94 (2.29–15.5) | | 0/161 | 0.0 (0.00–2.27) | | 8/538 | 1.49 (0.00–1.70) | |

*CI* confidence interval, *RFA* radiofrequency ablation, *TAE* trans-catheter arterial embolization

[a] Hospital volume was defined according to the number of cases per year. High hospital volume represents hospitals with more than 57 cases per year for hepatectomy, 105 cases per year for RFA, and 183 cases per year for TAE. Low hospital volume represents hospitals with fewer than 21 cases per year for hepatectomy, 38 cases per year for RFA, and 76 cases per year for TAE

In-hospital complications occurred in 763 (14.48 %), 531 (4.54 %) and 1,668 (4.49 %) for hepatectomy, RFA, and TAE patients, respectively. The details of the complications are listed in Table 3. Postoperative hemorrhage was the commonest complication of hepatectomy and was seen in 361 (6.85 %) admissions. The most significant complication of both RFA and TAE was related to bile duct stenosis, which occurred in 152 (1.30 %) and 657 (1.77 %) cases, respectively.

## Discussion

Hepatectomy, RFA, and TAE are widely applied therapeutic procedures which account for more than 90 % of all procedures performed in patients with primary HCC in Japan [23]. When deciding on a treatment strategy, both therapeutic efficacy and the risks associated with each treatment modality should be considered. Whereas the effectiveness of a procedure can be evaluated based on established criteria such as survival, local recurrence, and tumor necrosis, the complication rate as an index of safety varies greatly among reports, mainly because of differences in the definitions used. In-hospital mortality is a more reliable indicator of safety, but a large number of samples are required to obtain an accurate estimate of mortality, because death is a relatively rare event. In the present study, we investigated the mortalities and morbidities associated with various therapeutic procedures for HCC, using information from the nationally representative Japanese DPC database. It is particularly worth noting that the data for in-hospital mortality were expected to be 100 %

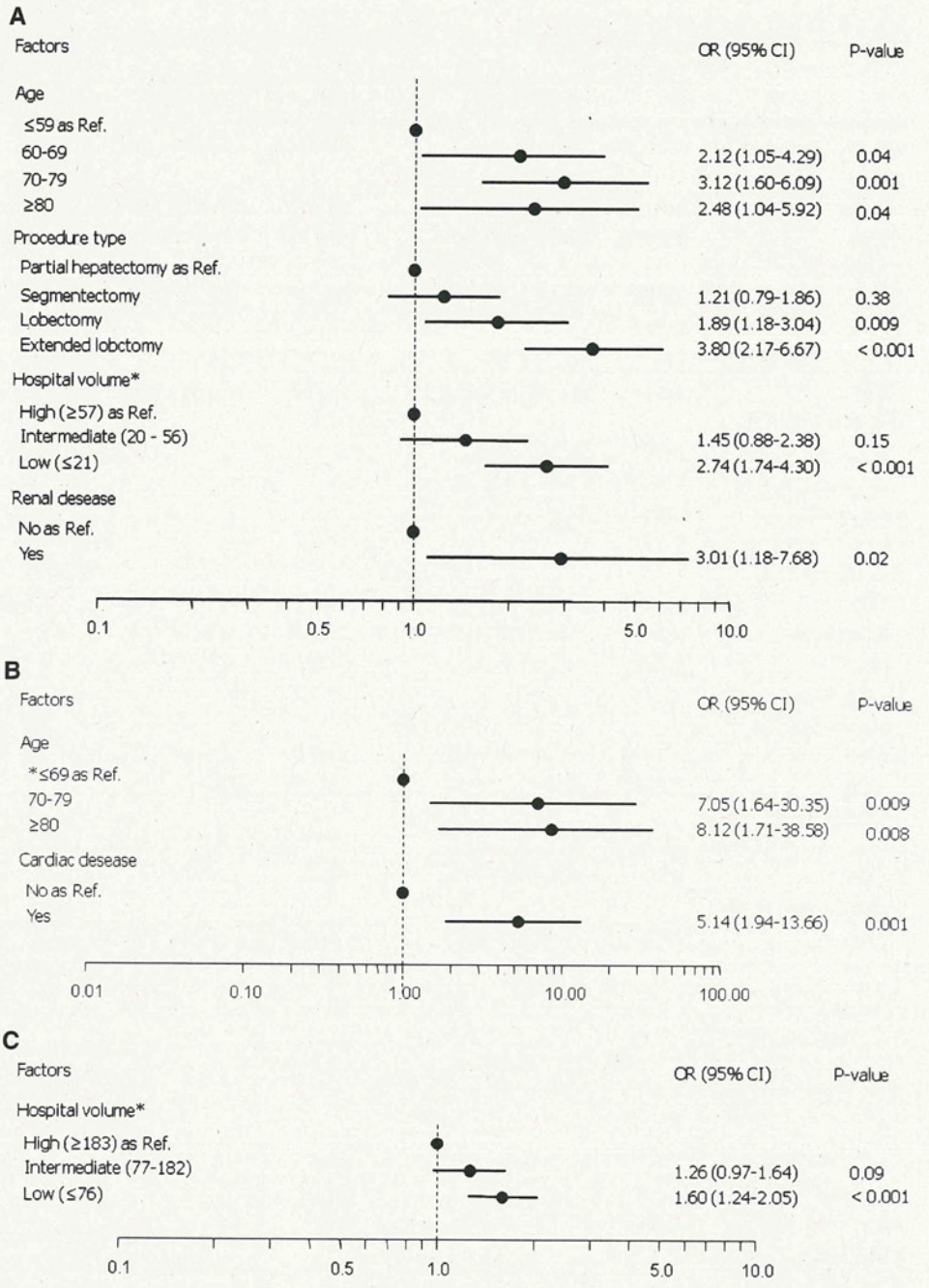


**Fig. 1** **a** Multivariate logistic regression analyses for in-hospital mortality of hepatectomy. **b** Multivariate logistic regression analyses for in-hospital mortality of radiofrequency ablation (RFA). *Asterisk* indicates that patients aged 60–69 years and those aged ≤59 years are combined because the mortality of the patients aged ≤59 years was 0. **c** Multivariate logistic regression analyses for in-hospital mortality of trans-catheter embolization (TAE). *OR* odds ratio, *CI* confidence interval, *Ref.* reference value

reliable and free from recall bias because outcome was a required item on discharge.

In this study, the mortality following hepatectomy was 2.60 %, out of a total of 54,145 patients with HCC. Previously reported in-hospital mortalities following hepatectomy for primary and metastatic liver tumors at major high-volume centers were 3.8–8 and 0–7.0 % [4, 5, 24–30], respectively. For example, one report from the United States, using data from a nationwide inpatient sample over a 9-year period, showed a mortality of 6 % [31]. However, the background of that study may be different from that of the present study; for example, lower invasive procedures such as partial hepatectomy and segmentectomy accounted for the major part of the present study. This kind of factor may have influenced the lower mortality rate in the present study.

The mortality associated with RFA in the present study was 0.25 %, which was similar to that noted in previous reports (0.2–0.6 %) [32–39]. Multivariate analysis identified older age and cardiac comorbidity as factors

**Table 3** Complications related to each procedure

| | Hepatectomy ($n = 5270$) | RFA ($n = 11688$) | TAE ($n = 37187$) |
|---|---|---|---|
| Overall, *n* (%)[a] | 763 (14.48) | 531 (4.54) | 1,668 (4.49) |
| Hemorrhage, *n* (%) | 361 (6.85) | 56 (0.48) | 102 (0.27) |
| Bile duct stenosis, *n* (%) | 59 (1.12) | 152 (1.30) | 657 (1.77) |
| Liver abscess, *n* (%) | 19 (0.36) | 36 (0.31) | 201 (0.54) |
| Pneumothorax, *n* (%) | 1 (0.02) | 16 (0.14) | – |
| Perforation of gastrointestinal tract, *n* (%) | 2 (0.04) | 3 (0.03) | – |
| Peritonitis, *n* (%) | 98 (1.86) | 98 (0.84) | – |
| Heat burn, *n* (%) | – | 7 (0.06) | – |
| Hepatic infarction, *n* (%) | – | 7 (0.06) | 3 (0.00) |
| Liver failure, *n* (%) | 122 (2.31) | 131 (1.12) | 617 (1.66) |
| Cardiac complication, *n* (%) | 35 (0.66) | 15 (0.13) | 37 (0.10) |
| Ruptured suture, *n* (%) | 40 (0.76) | 2 (0.02) | 2 (0.00) |
| Renal failure, *n* (%) | 26 (0.49) | 2 (0.02) | 35 (0.09) |
| Pulmonary embolism, *n* (%) | 7 (0.13) | 4 (0.03) | 14 (0.04) |
| Wound infection, *n* (%) | 12 (0.23) | 11 (0.09) | 11 (0.03) |
| Pneumonia, *n* (%) | 57 (1.08) | 30 (0.26) | 117 (0.31) |
| Allergy to anesthetic agents, *n* (%) | 2 (0.04) | 5 (0.04) | 86 (0.23) |

[a] More than one complication during hospitalization was counted as one

significantly related to high mortality in patients undergoing RFA.

A recent systematic review of the safety of TAE, based on 37 trials with 2,858 patients, reported a median periprocedural mortality (≤30 days) of 2.4 % (range 0–9.5 %) [40], which was higher than the in-hospital mortality for TAE in the present study (1.03 %). Some previous reports defined mortality as death within the 30 days following the procedure. In the present study, the 30-day mortalities for hepatectomy, RFA, and TAE were 1.08, 0.14, and 0.45 %, respectively.

A number of studies identified hospital procedure volume as an important determinant of postoperative mortality following advanced surgical procedures [31, 41–46]. In the present study, hospital procedure volume was significantly associated with in-hospital mortality for hepatectomy and TAE, but although the RFA-associated in-hospital mortality tended to be lower in high-volume hospitals, the difference was not significant. Despite the large sample size, it is still possible that this study was too underpowered to show any significant association between hospital volume and RFA mortality, because of the exceptionally low mortality rate of RFA. These results suggest that concentrating patients indicated for hepatectomy in high-volume centers should be considered on safety grounds.

In the present study, the mortality rate for hepatectomy was lower in patients over 80 years old. The indication for hepatectomy is determined on the basis of several factors. Although there is no specific age limitation for hepatectomy in Japan, older patients have shorter long-term survival after hepatectomy compared to younger patients, because of their expected life span. Thus, the indication for hepatectomy in older patients, especially those over 80, is stricter in clinical practice. Taking these factors into consideration, it is possible that the patients over 80 years old from the DPC database who did undergo hepatectomy were in generally better than average health. That could explain the lower mortality associated with hepatectomy in patients of 80 years and over in the present study. Similarly, the in-hospital mortality rate for TAE was significantly lower in older patients according to the univariate analysis. This result also may be related to the indications for TAE in Japan. Moreover, the intensity and area of embolization for TAE can be regulated, and embolization is likely to be less intensive in older patients, possibly accounting for the lower mortality in older patients who underwent TAE. Cardiac comorbidity was significantly associated with in-hospital mortality for RFA. According to the database, three out of the five deceased patients with cardiac comorbidities were speculated to have died as a result of cardiac complications (e.g., myocardial infarction, angina pectoris, and heart failure). RFA is thought to be less invasive than hepatectomy, and is sometimes considered as an alternative therapy to hepatectomy in patients with relatively severe cardiac comorbidities. The cardiac comorbidities were thus likely to have been severe in the RFA group, which could account for the higher mortality after RFA in the present study.

The complication rates for hepatectomy, RFA, and TAE in the present study were 14.48, 4.54, and 4.49 %, respectively. Previously reported complication rates have varied among studies, ranging from 28.4 to 47.7 % [47–

52], from 0 to 12.7 % [32–38], and from 4.3 to 10.8 % [53–55] for hepatectomy, RFA, and TAE, respectively. Our multivariate logistic regression analysis demonstrated that the complication rate was significantly higher after more invasive procedures in patients treated in hospitals with lower procedure volumes, in patients with diabetes mellitus, and in patients with cardiac diseases in the case of hepatectomy; and in patients treated in hospitals with higher procedure volumes, patients with diabetes mellitus, and patients with cardiac diseases for RFA and TAE (data not shown). However, complications are usually reported in the DPC database in relation to the reimbursement of medical fees, and the reported complications were therefore less objective than the reported mortality, and could have been underestimated. The complication rate was relatively low for hepatectomy, and the rates for the other procedures were similar to those in previous reports.

The present study had several limitations. First, although the DPC database represents approximately 40 % of all admissions to secondary and tertiary care hospitals in Japan, participating hospitals tend to be medium-to-large-sized institutions. The mortality could therefore have been underestimated by potentially excluding low-procedure-volume hospitals. Second, some important clinical data that may affect the risk of death related to treatments, such as the size and location of the tumor, and severity indexes of liver disease [e.g., the Child–Pugh and model for end-stage liver disease (MELD) scores] were unavailable in this database. Third, data on late-onset complications that appeared after discharge (i.e., biloma, biliary injury, or hepatic abscess) were also unavailable, because the database covers only inpatient data. This may have led to an underestimation of the complication rate in this study. However, according to previous reports, late-onset complications appear to have minimal effects on the mortality rates. Fourth, as noted above, as the DPC system was basically designed for assessing reimbursement, co-existing diseases are usually reported when a specific treatment is needed,; e.g., the proportion of patients with diabetes was higher in the hepatectomy group than that with the other procedures. This may be because patients who underwent hepatectomy were more likely to have been treated with intensive insulin therapy before surgery. Fifth, the immediate cause of death is not a required item in the DPC database. Accordingly, the in-hospital deaths recorded in this database have room for treatment unrelated deaths, the procedure-related mortality could therefore have been overestimated. However in-hospital mortality is more robust in terms of objectivity compared to treatment-related mortality assessed by operators. Finally, some complications, such as tumor seeding, were not covered by the ICD codes and could therefore not be evaluated.

In conclusion, this study confirmed that the therapeutic procedures used to treat liver tumors in Japan were associated with low mortalities and low complication rates. However, procedure-related mortality can be affected by patient and therapeutic backgrounds.

**Acknowledgments** This work was supported by a Grant-in-Aid for Research on Policy Planning and Evaluation from the Ministry of Health, Labour and Welfare, Japan; and Health Sciences Research Grants of The Ministry of Health, Labour and Welfare (Research on Hepatitis).

**Conflict of interest** The authors declare that they have no conflict of interest.

## References

1. Jemal A, Murray T, Ward E, Samuels A, Tiwari RC, Ghafoor A, et al. Cancer statistics, 2005. CA Cancer J Clin. 2005;55:10–30.
2. Kamangar F, Dores GM, Anderson WF. Patterns of cancer incidence, mortality, and prevalence across five continents: defining priorities to reduce cancer disparities in different geographic regions of the world. J Clin Oncol. 2006;24:2137–50.
3. Arii S, Yamaoka Y, Futagawa S, Inoue K, Kobayashi K, Kojiro M, et al. Results of surgical and nonsurgical treatment for small-sized hepatocellular carcinomas: a retrospective and nationwide survey in Japan. The Liver Cancer Study Group of Japan. Hepatology. 2000;32:1224–9.
4. Fong Y, Sun RL, Jarnagin W, Blumgart LH. An analysis of 412 cases of hepatocellular carcinoma at a Western center. Ann Surg. 1999;229:790–9 (discussion 799–800).
5. Grazi GL, Ercolani G, Pierangeli F, Del Gaudio M, Cescon M, Cavallari A, et al. Improved results of liver resection for hepatocellular carcinoma on cirrhosis give the procedure added value. Ann Surg. 2001;234:71–8.
6. Llovet JM, Fuster J, Bruix J. Intention-to-treat analysis of surgical treatment for early hepatocellular carcinoma: resection versus transplantation. Hepatology. 1999;30:1434–40.
7. Takayama T, Makuuchi M, Hirohashi S, Sakamoto M, Yamamoto J, Shimada K, et al. Early hepatocellular carcinoma as an entity with a high rate of surgical cure. Hepatology. 1998;28:1241–6.
8. Abdalla EK, Vauthey JN, Ellis LM, Ellis V, Pollock R, Broglio KR, et al. Recurrence and outcomes following hepatic resection, radiofrequency ablation, and combined resection/ablation for colorectal liver metastases. Ann Surg. 2004;239:818–25. discussion 825–17.
9. Choti MA, Sitzmann JV, Tiburi MF, Sumetchotimetha W, Rangsin R, Schulick RD, et al. Trends in long-term survival following liver resection for hepatic colorectal metastases. Ann Surg. 2002;235:759–66.
10. Fernandez FG, Drebin JA, Linehan DC, Dehdashti F, Siegel BA, Strasberg SM. Five-year survival after resection of hepatic metastases from colorectal cancer in patients screened by positron emission tomography with F-18 fluorodeoxyglucose (FDG-PET). Ann Surg. 2004;240:438–47 (discussion 447–50).
11. Rossi S, Di Stasi M, Buscarini E, Quaretti P, Garbagnati F, Squassante L, et al. Percutaneous RF interstitial thermal ablation in the treatment of hepatic cancer. AJR Am J Roentgenol. 1996;167:759–68.
12. Livraghi T, Goldberg SN, Lazzaroni S, Meloni F, Solbiati L, Gazelle GS. Small hepatocellular carcinoma: treatment with radio-frequency ablation versus ethanol injection. Radiology. 1999;210:655–61.

13. Curley SA, Izzo F, Delrio P, Ellis LM, Granchi J, Vallone P, et al. Radiofrequency ablation of unresectable primary and metastatic hepatic malignancies: results in 123 patients. Ann Surg. 1999;230:1–8.
14. Tateishi R, Shiina S, Teratani T, Obi S, Sato S, Koike Y, et al. Percutaneous radiofrequency ablation for hepatocellular carcinoma. An analysis of 1000 cases. Cancer. 2005;103:1201–9.
15. Bruix J, Sherman M. Management of hepatocellular carcinoma. Hepatology. 2005;42:1208–36.
16. Chang MH, You SL, Chen CJ, Liu CJ, Lee CM, Lin SM, et al. Decreased incidence of hepatocellular carcinoma in hepatitis B vaccinees: a 20-year follow-up study. J Natl Cancer Inst. 2009;101:1348–55.
17. Llovet JM, Bruix J. Systematic review of randomized trials for unresectable hepatocellular carcinoma: chemoembolization improves survival. Hepatology. 2003;37:429–42.
18. Imamura H, Seyama Y, Kokudo N, Maema A, Sugawara Y, Sano K, et al. One thousand fifty-six hepatectomies without mortality in 8 years. Arch Surg. 2003;138:1198–206 (discussion 1206).
19. Jarnagin WR, Gonen M, Fong Y, DeMatteo RP, Ben-Porat L, Little S, et al. Improvement in perioperative outcome after hepatic resection: analysis of 1,803 consecutive cases over the past decade. Ann Surg. 2002;236:397–406 (discussion 397–406).
20. Sumitani M, Uchida K, Yasunaga H, Horiguchi H, Kusakabe Y, Matsuda S, et al. Prevalence of malignant hyperthermia and relationship with anesthetics in Japan: data from the diagnosis procedure combination database. Anesthesiology. 2011;114:84–90.
21. Yasunaga H, Shi Y, Takeuchi M, Horiguchi H, Hashimoto H, Matsuda S, et al. Measles-related hospitalizations and complications in Japan, 2007–2008. Intern Med. 2010;49:1965–70.
22. Yasunaga H, Yanaihara H, Fuji K, Horiguchi H, Hashimoto H, Matsuda S. Impact of hospital volume on postoperative complications and in-hospital mortality after renal surgery: data from the Japanese Diagnosis Procedure Combination Database. Urology. 2010;76:548–52.
23. Ikai I, Arii S, Okazaki M, Okita K, Omata M, Kojiro M, et al. Report of the 17th nationwide follow-up survey of primary liver cancer in Japan. Hepatol Res. 2007;37:676–91.
24. Belghiti J, Regimbeau JM, Durand F, Kianmanesh AR, Dondero F, Terris B, et al. Resection of hepatocellular carcinoma: a European experience on 328 cases. Hepatogastroenterology. 2002;49:41–6.
25. Biasco G, Gallerani E. Treatment of liver metastases from colorectal cancer: what is the best approach today? Dig Liver Dis. 2001;33:438–44.
26. Cromheecke M, de Jong KP, Hoekstra HJ. Current treatment for colorectal cancer metastatic to the liver. Eur J Surg Oncol. 1999;25:451–63.
27. Poon RT, Fan ST. Hepatectomy for hepatocellular carcinoma: patient selection and postoperative outcome. Liver Transpl. 2004;10:S39–45.
28. Ruers T, Bleichrodt RP. Treatment of liver metastases, an update on the possibilities and results. Eur J Cancer. 2002;38:1023–33.
29. Vivarelli M, Guglielmi A, Ruzzenente A, Cucchetti A, Bellusci R, Cordiano C, et al. Surgical resection versus percutaneous radiofrequency ablation in the treatment of hepatocellular carcinoma on cirrhotic liver. Ann Surg. 2004;240:102–7.
30. Yoon SS, Tanabe KK. Multidisciplinary management of metastatic colorectal cancer. Surg Oncol. 1998;7:197–207.
31. Kohn GP, Nikfarjam M. The effect of surgical volume and the provision of residency and fellowship training on complications of major hepatic resection. J Gastrointest Surg. 2010;14:1981–9.
32. Bilchik AJ, Wood TF, Allegra DP. Radiofrequency ablation of unresectable hepatic malignancies: lessons learned. Oncologist. 2001;6:24–33.
33. Curley SA, Izzo F, Ellis LM, Nicolas Vauthey J, Vallone P. Radiofrequency ablation of hepatocellular cancer in 110 patients with cirrhosis. Ann Surg. 2000;232:381–91.
34. de Baere T, Risse O, Kuoch V, Dromain C, Sengel C, Smayra T, et al. Adverse events during radiofrequency treatment of 582 hepatic tumors. AJR Am J Roentgenol. 2003;181:695–700.
35. Giorgio A, Tarantino L, de Stefano G, Coppola C, Ferraioli G. Complications after percutaneous saline-enhanced radiofrequency ablation of liver tumors: 3-year experience with 336 patients at a single center. AJR Am J Roentgenol. 2005;184:207–11.
36. Jansen MC, van Duijnhoven FH, van Hillegersberg R, Rijken A, van Coevorden F, van der Sijp J, et al. Adverse effects of radiofrequency ablation of liver tumours in the Netherlands. Br J Surg. 2005;92:1248–54.
37. Livraghi T, Solbiati L, Meloni MF, Gazelle GS, Halpern EF, Goldberg SN. Treatment of focal liver tumors with percutaneous radio-frequency ablation: complications encountered in a multicenter study. Radiology. 2003;226:441–51.
38. Wood TF, Rose DM, Chung M, Allegra DP, Foshag LJ, Bilchik AJ. Radiofrequency ablation of 231 unresectable hepatic tumors: indications, limitations, and complications. Ann Surg Oncol. 2000;7:593–600.
39. Kasugai H, Osaki Y, Oka H, Kudo M, Seki T. Severe complications of radiofrequency ablation therapy for hepatocellular carcinoma: an analysis of 3,891 ablations in 2,614 patients. Oncology. 2007;72(Suppl 1):72–5.
40. Marelli L, Stigliano R, Triantos C, Senzolo M, Cholongitas E, Davies N, et al. Transarterial therapy for hepatocellular carcinoma: which technique is more effective? A systematic review of cohort and randomized studies. Cardiovasc Interv Radiol. 2007;30:6–25.
41. Begg CB, Cramer LD, Hoskins WJ, Brennan MF. Impact of hospital volume on operative mortality for major cancer surgery. JAMA. 1998;280:1747–51.
42. Birkmeyer JD, Siewers AE, Finlayson EV, Stukel TA, Lucas FL, Batista I, et al. Hospital volume and surgical mortality in the United States. N Engl J Med. 2002;346:1128–37.
43. Birkmeyer JD, Stukel TA, Siewers AE, Goodney PP, Wennberg DE, Lucas FL. Surgeon volume and operative mortality in the United States. N Engl J Med. 2003;349:2117–27.
44. Birkmeyer JD, Sun Y, Goldfaden A, Birkmeyer NJ, Stukel TA. Volume and process of care in high-risk cancer surgery. Cancer. 2006;106:2476–81.
45. Kuwabara K, Matsuda S, Fushimi K, Ishikawa KB, Horiguchi H, Fujimori K. Impact of hospital case volume on the quality of laparoscopic colectomy in Japan. J Gastrointest Surg. 2009;13:1619–26.
46. Schrag D, Cramer LD, Bach PB, Cohen AM, Warren JL, Begg CB. Influence of hospital procedure volume on outcomes following surgery for colon cancer. JAMA. 2000;284:3028–35.
47. Benzoni E, Cojutti A, Lorenzin D, Adani GL, Baccarani U, Favero A, et al. Liver resective surgery: a multivariate analysis of postoperative outcome and complication. Langenbecks Arch Surg. 2007;392:45–54.
48. Delis SG, Bakoyiannis A, Dervenis C, Tassopoulos N. Perioperative risk assessment for hepatocellular carcinoma by using the MELD score. J Gastrointest Surg. 2009;13:2268–75.
49. Laurent C, Sa Cunha A, Couderc P, Rullier E, Saric J. Influence of postoperative morbidity on long-term survival following liver resection for colorectal metastases. Br J Surg. 2003;90:1131–6.
50. Schiesser M, Chen JW, Maddern GJ, Padbury RT. Perioperative morbidity affects long-term survival in patients following liver resection for colorectal metastases. J Gastrointest Surg. 2008;12:1054–60.
51. Sim HG, Ooi LL. Results of resections for hepatocellular carcinoma in a new hepatobiliary unit. ANZ J Surg. 2003;73:8–13.

52. Ziparo V, Balducci G, Lucandri G, Mercantini P, Di Giacomo G, Fernandes E. Indications and results of resection for hepatocellular carcinoma. Eur J Surg Oncol. 2002;28:723–8.
53. Kiely JM, Rilling WS, Touzios JG, Hieb RA, Franco J, Saeian K, et al. Chemoembolization in patients at high risk: results and complications. J Vasc Interv Radiol. 2006;17:47–53.
54. Kothary N, Weintraub JL, Susman J, Rundback JH. Transarterial chemoembolization for primary hepatocellular carcinoma in patients at high risk. J Vasc Interv Radiol. 2007;18:1517–26 (quiz 1527).
55. Pietrosi G, Miraglia R, Luca A, Vizzini GB, Fili D, Riccardo V, et al. Arterial chemoembolization/embolization and early complications after hepatocellular carcinoma treatment: a safe standardized protocol in selected patients with Child class A and B cirrhosis. J Vasc Interv Radiol. 2009;20:896–902.

SCIENTIFIC REPORTS

OPEN

SUBJECT AREAS:
MOLECULAR BIOLOGY
CELL BIOLOGY
GENE REGULATION
INNATE IMMUNITY

Received
25 July 2012

Accepted
14 August 2012

Published
6 September 2012

Correspondence and requests for materials should be addressed to M.O. (otsukamo-tky@umin.ac.jp)

* These authors contributed equally to this work.

# Silencing of microRNA-122 enhances interferon-α signaling in the liver through regulating SOCS3 promoter methylation

Takeshi Yoshikawa*, Akemi Takata*, Motoyuki Otsuka*, Takahiro Kishikawa, Kentaro Kojima, Haruhiko Yoshida & Kazuhiko Koike

Department of Gastroenterology, Graduate School of Medicine, The University of Tokyo, Tokyo 113-8655, Japan.

**Hepatitis C virus (HCV) infection is a major cause of chronic liver disease worldwide. Although novel drugs against HCV are under development, the current standard therapy consists principally of interferon (IFN). To improve the response to IFN treatment by enhancing interferon-stimulated response element (ISRE)-mediated gene transcription, we screened 75 microRNAs highly expressed in hepatocytes for their ability to modulate ISRE activity. Overexpression of microRNA-122 (miR122) significantly suppressed ISRE activity. Conversely, silencing of miR122 function enhanced IFN-induced ISRE activity, by decreasing expression of suppressor of cytokine signaling 3 (SOCS3). This decrease in SOCS3 level was not mediated by microRNA target gene suppression, but rather by enhanced methylation at SOCS3 gene promoter. Taken together, our data, along with the fact that antisense oligonucleotides of miR122 also directly inhibit HCV replication, suggest that a combination therapy comprising IFN and silencing of miR122 function may be a promising therapeutic option in the near future.**

More than 170 million individuals worldwide are chronically infected with hepatitis C virus (HCV), which results in hepatic inflammation, hepatic fibrosis, and liver cirrhosis[1]. End-stage liver diseases as well as hepatocellular carcinoma attributable to chronic hepatitis C are increasingly serious problems[2]. For almost a decade, the standard of care in patients with chronic hepatitis C has consisted of pegylated interferon-α2a (pegIFN-α2a) or pegIFN-α2b in combination with the guanosin analog ribavirin. However, this eradicates HCV in only about half of those infected with HCV genotype 1, the most common genotype globally. Moreover, severe adverse events are associated with IFN therapy, such as myelo-suppression and flu-like syndrome. Because these effects are dose-limiting, many patients are unable to receive a higher dose of IFN that might more effectively inhibit HCV replication[3]. While recent licensing of HCV protease inhibitors for the treatment of patients with chronic hepatitis C as part of a triple therapy with pegIFN-α and ribavirin is expected to increase the sustained viral response (SVR) rate, IFN currently remains the principal drug for the eradication of HCV.

Type I interferons (IFNs), such as IFN-α and IFN-β, bind to the type I IFN receptor[4]. One major pathway in type I IFN signaling involves the Jak-STAT signaling cascade[5]. Activated tyrosine kinases phosphorylate STAT-1 and STAT-2 proteins, which bind to p48, a member of the IFN regulatory family (IRF), to form interferon-stimulated gene factor-3 (ISGF3). ISGF3 translocates to the nucleus and binds to the interferon-stimulated response element (ISRE) in the promoter region of IFN target genes, which code for antiviral proteins such as double-stranded RNA-activated protein kinase (PKR) and 2′5′-oligoadenylate synthethase (OAS1). On the other hand, regulatory molecules are also involved in the IFN pathway. The suppressor of cytokine signaling (SOCS) protein is a negative regulator of the Jak-STAT cascade[6]. The SOCS family includes eight members (SOCS-1 to SOCS-7 and CIS), all sharing a central SH2 domain and a C-terminal SOCS box. SOCS-1 and SOCS-3 are the most effective members of this family, and act as negative regulators of several intracellular pathways, particularly the Jak–STAT pathway. In hepatic cells, inhibition of IFN-α-induced STAT-1 activation by HCV core protein overexpression is associated with induction of SOCS-3 mRNA expression[7]. Therefore, increased SOCS3 protein expression during HCV infection may be a mechanism of IFN resistance[8–10]. Such regulatory functions may also be important determinants of the efficacy of anti-HCV IFN therapy.

MicroRNAs are short, single-stranded, non-coding RNAs. They are expressed in most organisms, ranging from plants to vertebrates[11], and are involved in the regulation of target gene expression. Different microRNAs are responsible for the control of various biological processes[12–14]. In this context, a number of microRNAs have

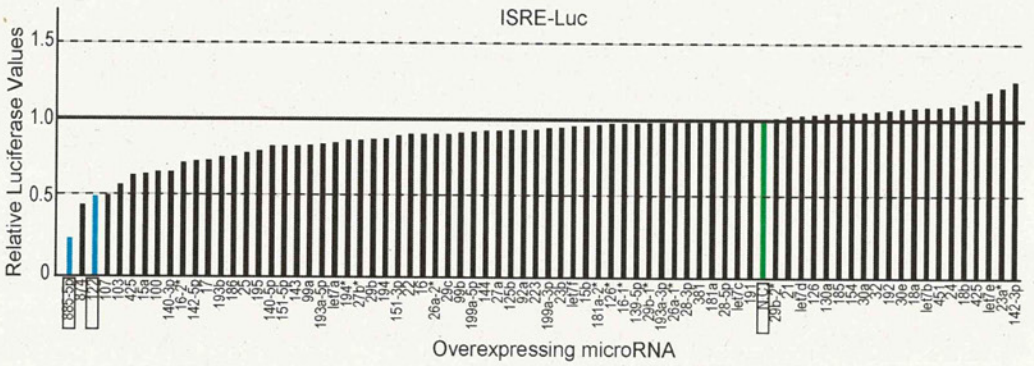


**Figure 1 | MiR122 and miR885-5p suppress ISRE activity.** Functional screening for liver microRNAs that modulate ISRE activity. Seventy-five mature microRNA oligonucleotides known to be highly expressed in the liver were transiently reverse-transfected into stable 293T cell-derived ISRE reporter cell lines, followed by IFN-α stimulation. Reporter activities were normalized to the values of negative control RNA oligonucleotides (N.C. in green) and ranked in ascending order. Determinations were performed in duplicate, and a representative result is shown. MiR122 and miR885-5p, which were chosen for further analyses, are in blue and represented as rectangles.

recently been shown to regulate the function of intracellular signaling intermediates, such as p53 and NF-κB pathways, by regulating expression of their target genes[15–18].

Primary microRNAs, which possess stem-loop structures, are processed into mature microRNAs by Drosha and Dicer RNA polymerase III. These mature microRNAs then associate with the RNA-induced silencing complex (RISC), and the resulting complex binds directly to the 3′-untranslated regions (3′-UTRs) of target mRNAs to suppress translation and gene expression post-transcriptionally. While this is undoubtedly the main action of microRNAs, recent studies have demonstrated that microRNAs can enter the nucleus[19], and are involved in establishing DNA methylation[20–22]. In addition, microRNAs may also regulate chromatin structure by regulating key histone modifiers[23]. Taken together, these results suggest that microRNAs are important players in epigenetic and post-transcriptional control of gene expression[20].

The aim of this study was to determine the possible role of microRNAs in IFN signaling. We focused on microRNAs expressed in the liver because we were interested in regulators of IFN signaling during HCV treatment. We screened a subset of microRNAs for their ability to modulate ISRE activity to develop a more effective IFN-based therapy against chronic hepatitis C infection.

## Results

**Screening for microRNAs regulating ISRE activities.** We initially screened for microRNAs that affected ISRE-mediated gene transcription using stable ISRE activity reporter cell lines and by transiently overexpressing 75 mature synthetic microRNAs, as we did previously to screen for microRNAs that affect NF-κB activity[15]. Because we were interested in IFN-mediated intracellular signaling in the liver, the microRNAs examined were selected on the basis of their hepatic expression level[24]. In addition, we used non-liver 293T cells for the initial screening to determine the effects of the microRNA overexpression. The data suggested differential effects of microRNAs on ISRE activity in response to IFN-α stimulation (Fig. 1). Of the microRNAs examined, we chose miR122 and miR885-5p for further investigation because they suppressed ISRE activity significantly and reproducibly in two independent screens.

**Silencing of miR122 enhances ISRE activities.** To confirm the suppressive effects of miR122 and miR885 overexpression on ISRE activities, we first performed a reporter assay to monitor ISRE activities with plasmid-based miR-overexpressing constructs. While both miR122 and miR885 suppressed ISRE activities induced by IFN-α stimulation in 293T cells, the effect of miR122 was more significant (Fig. 2a). For this reason, and because miR122 is the most abundant microRNA in the liver[24], we further focused on miR122. The suppressive effect of miR122 was ISRE-specific, because it had no effect on p53-mediated transcriptional activities (Fig. 2b). Next, to examine the effects of silencing miR122 function on ISRE activity in hepatoma cell lines, we transiently transfected plasmid-based anti-miR122 constructs into Huh7 cells, in which miR122 is highly expressed[25]. The silencing of miR122 function resulted in about two-fold augmentation of IFN-α-induced ISRE activity (Fig. 2c), suggesting that miR122 is also involved in ISRE activity in hepatoma cell lines during IFN-α treatment. To further confirm these effects, we examined Hela-Tet-Off-miR122 cells, in which the expression of miR122 precursors can be shut off by doxycyclin treatment. In these cells, ISRE activity was more highly induced by IFN-α treatment when the expression of miR122 precursors was suppressed by doxycyclin treatment (Fig. 2d). Interferon stimulated genes, such as ISG15 and IFNAR1, were induced to a greater extent by IFN-α treatment in miR122-silenced Huh7 cells than in control cells (Fig. 2e and 2f). These data suggest that silencing miR122 can enhance IFN-α-ISRE activities.

**Silencing miR122 suppresses SOCS3 expression by methylation of its promoter.** To gain insight into the mechanisms underlying the suppression of ISRE activity by miR122, we searched the Gene Expression Omnibus (GEO) database regarding the effect of silencing miR122 on changes in IFN pathway-related gene expression (DataSet Record GDS1729)[26]. Consistent with our results (Fig. 2), the expression of several known ISRE-mediated IFN-stimulated genes, such as OAS1, interferon α and β receptor 1 (Ifnar1), interferon α-inducible protein 27-like 2A (Ifi27l2a), and interferon regulatory factor 6 (IRF6), were indeed up-regulated by silencing miR122 function in the mouse liver. However, the expression of regulatory genes involved in the IFN signaling pathway from the receptor to the nucleus, such as STAT1, STAT2, JAK1, and JAK2, were unchanged. Although we searched for potential miR122 target genes related to IFN signaling in several microRNA target databases, including TargetScan (http://www.targetscan.org), no major IFN-related genes were found.

Because epigenetic changes induced by microRNAs have been reported[20–22], we compared the comprehensive methylation levels of 27,578 promoter-associated CpG sites using an Illumina Infinium methylation assay (Human Methylation27 BeadChip) between control and stably miR122-silenced Huh7 cell lines. Although the methylation levels of most CpG sites were unchanged, those of a number of CpG sites were altered by silencing miR122 (Table 1). While the methylation of most of these decreased, the CpG sites of a few genes were more methylated by miR122 silencing. The most

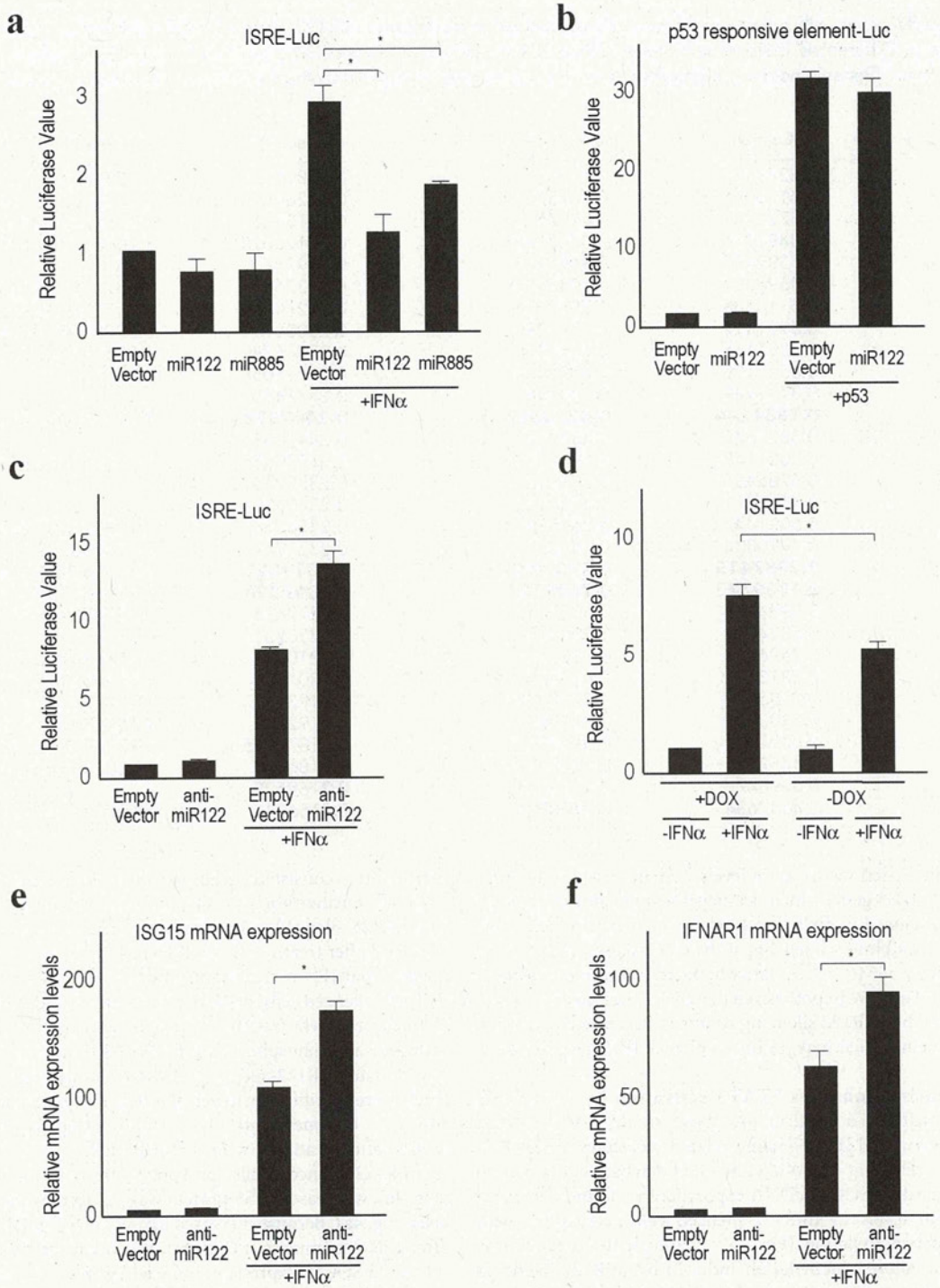


**Figure 2 | MiR122 modulates ISRE activities.** (a) Overexpression of the selected microRNA precursors suppresses ISRE activity following IFN-α stimulation. ISRE reporter plasmids were transiently transfected, with or without selected microRNA precursor-expressing plasmids, into Huh7 cells. Luciferase values were normalized to those of cells transfected with an empty vector and without IFN, which were set to 1. *, $p < 0.05$. Data represent the means ± standard deviations (SD) of three independent determinations. Similar results were obtained using HepG2 cells. (b) p53 activities were unaffected by miR122 expression. Reporter assays were performed with p53 reporter and p53 expressing plasmids with or without miR122 precursor expression in Huh7 cells. Data represent the means ± SD of three independent determinations. (c) Silencing of miR122 function enhances ISRE activity. Anti-miR122 expressing plasmids were used to perform an ISRE reporter assay in Huh7 cells. *, $p < 0.05$. Data represent the means ± SD of three independent determinations. (d) Hela-Tet-Off-miR122 precursor cell lines were used to measure ISRE activity. Cells were transfected with ISRE reporter constructs with (DOX+) or without (DOX-) doxycyclin. DOX+ shut off the miR122 expression in these cells. The reporter activities after 6 h of IFN-α stimulation were compared. *, $p < 0.05$. Data represent the means ± SD of three independent determinations. (e, f) IFN-inducible genes (e, ISG15; f, IFNAR1) were more induced in miR122-silenced Huh7 cells, determined by quantitative RT-PCR using RNA after 6 h of IFN-α stimulation. *, $p < 0.05$. Data represent the means ± SD of three independent determinations.

Table 1 | Top 30 genes with promoters differentially methylated in control and miR122-silenced Huh7 cells. Values indicate methylation levels. Values in 'Differences' indicate quantitative differences in methylation levels of target gene CpG sites. Higher values indicate greater methylation levels. Genes in bold and highlighted in gray means greater methylation; others were less methylated in miR122-silenced Huh7 cells

| SYMBOL | Control | miR122-silenced | Difference | CpG ISLAND LOCATIONS |
|---|---|---|---|---|
| GPC3 | 0.4242135 | 0.11596 | 0.3082535 | X:132946499-132947763 |
| FLJ30058 | 0.4155016 | 0.1428133 | 0.2726883 | X:130019792-130020537 |
| EIF3S6IP | 0.672594 | 0.4012034 | 0.2713906 | 22:36574299-36576077 |
| BHLHB9 | 0.3481071 | 0.07687688 | 0.27123022 | X:101862184-101862707 |
| PORCN | 0.6389685 | 0.3697215 | 0.269247 | |
| MSI2 | 0.4593301 | 0.1955636 | 0.2637665 | 17:52688030-52689554 |
| DNTT | 0.6114385 | 0.3489618 | 0.2624767 | 10:98054238-98054478 |
| SEMA3B | 0.3901392 | 0.1301293 | 0.2600099 | 3:50285369-50286362 |
| RYR2 | 0.4331115 | 0.1756537 | 0.2574578 | 1:235271651-235273428 |
| TCEAL7 | 0.6519198 | 0.4006093 | 0.2513105 | |
| NR0B2 | 0.3711949 | 0.1234481 | 0.2477468 | |
| **SOCS3** | **0.1831344** | **0.4273662** | **0.2442318** | 17:73866027-73868731 |
| TAS2R16 | 0.5821649 | 0.3380581 | 0.2441068 | |
| BHLHB9 | 0.3021148 | 0.06171004 | 0.24040476 | X:101862184-101862707 |
| OR12D3 | 0.5266486 | 0.2884241 | 0.2382245 | |
| ADAMTSL1 | 0.4537211 | 0.2196532 | 0.2340679 | |
| TBX6 | 0.5031447 | 0.2695281 | 0.2336166 | 16:30010427-30011656 |
| ICAM4 | 0.4990334 | 0.2668367 | 0.2321967 | 19:10258558-10259935 |
| **C9orf125** | **0.2387415** | **0.4707038** | **0.2319623** | 9:103287963-103289481 |
| **ELN** | **0.1332373** | **0.3629701** | **0.2297328** | 7:73080116-73080605 |
| ANKRD30A | 0.898423 | 0.6711555 | 0.2272675 | 10:37453955-37454965 |
| OR10J1 | 0.5324367 | 0.3094136 | 0.2230231 | |
| TP73 | 0.3596564 | 0.1386476 | 0.2210088 | 1:3596889-3597535 |
| CNNM1 | 0.6313883 | 0.4106784 | 0.2207099 | 10:101078809-101080801 |
| DHH | 0.2955738 | 0.07619943 | 0.21937437 | 12:47774151-47774653 |
| CTAG2 | 0.5303309 | 0.3110451 | 0.2192858 | X:153536438-153536702 |
| GNB4 | 0.3091451 | 0.09039365 | 0.21875145 | 3:180651316-180652496 |
| PNPLA2 | 0.4458646 | 0.2272328 | 0.2186318 | 11:808884-809164 |
| FGF7 | 0.6298472 | 0.4128944 | 0.2169528 | |
| NTE | 0.4557684 | 0.2400911 | 0.2156773 | 19:7504300-7507429 |

significantly increased methylation levels were observed in the promoter of the SOCS3 gene, which is a negative regulator of IFN signaling. The enhanced methylation levels in silencing miR122 were confirmed by bisulphite sequencing at the CpG island in the SOCS3 promoter, from −556 to −335 relative to the transcriptional start site (Fig. 3a and b). Thus, we hypothesized that the greater methylation of SOCS3 induced by miR122 silencing results in decreased expression of SOCS3 protein, which may, in turn, enhance IFN-α signaling.

**MiR122 silencing enhances STAT3 activation by decreasing SOCS3 expression.** To confirm the above results, we examined SOCS3 expression and IFN signaling-related molecules in miR122-silenced Huh7 cells (Fig 4a). While the GEO database contained no direct data regarding SOCS3 cDNA expression, we found decreased SOCS3 protein levels in miR122-silenced cells, consistent with promoter hyper-methylation (Fig. 4a). Although the mechanisms underlying the altered methylation induced by miR122 silencing remain unknown, it did not depend on DNA methyltransferase 1 (Dnmt1), which is a key mediator of DNA methylation that catalyzes the methylation of CpG dinucleotides in genomic DNA[27], because the decreased SOCS3 expression by miR122 silencing was also present in Dnmt1 knockdown cells (Fig. 4b).

Because SOCS3 is a potent inhibitor of STAT3 activation[6], and because type I IFNs induce STAT3 as well as STAT1 and STAT2 activation[5,28], we examined the phosphorylation status of STAT proteins after IFN treatment in Huh7 control and miR122-silenced cells (Fig. 4a). While the STAT1, 2, and 3 protein levels and the phosphorylation levels of STAT1 before and after IFN-α stimulation in these two cell lines did not differ significantly, STAT3 phosphorylation levels were higher in miR122-silenced cells 1 and 6 h after IFN-α stimulation, consistent with the decreased expression of SOCS3 (Fig. 4a). Furthermore, STAT2 phosphorylation was slightly higher in miR122-silenced cells (Fig. 4a). Similar tendencies were also observed after treatment with IFN-β, another type I IFN. These data suggest that IFN-α treatment induced greater STAT3 activation in miR122-silenced cells, probably due to decreased SOCS3 expression.

In contrast, whereas IFN-γ (type II IFN) and IFN-λ (type III IFN) induced slight phosphorylation of STAT1 and STAT3, the levels in control and miR122-silenced cells were comparable. STAT2 protein levels were significantly lower in miR122-silenced cells than in controls after treatment with these cytokines (Fig. 4a). No induction of SOCS3 after treatment with IFN-α/β, IFN-γ, or IFN-λ was detected in miR122-silenced cells, probably due to promoter methylation (Fig. 4a), whereas SOCS3 protein was induced by all IFNs in control cells (Fig. 4a). Because increased expression of miR122 was detected after IFN-λ stimulation (Fig. 4c), this might be responsible for the increased SOCS3 expression induced by IFN-λ stimulation.

To confirm whether the induction of the enhanced ISRE activity in miR122-silencing was dependent on the decreased expression of SOCS3, we investigated whether the restoration of SOCS3 expression in miR122-silencing could reduce the ISRE activity in a reporter assay. The overexpression of SOCS3 in miR122-silenced Huh7 cells reduced the induction of ISRE activity caused by miR122-silencing (Fig. 5a and b), although we could not fully exclude the possibility that other mechanisms were also involved because the reversal of ISRE activity did not completely reach the level of the control. To support this, we confirmed the restoration of STAT2 and STAT3 phosphorylation levels induced by IFN-α treatment in miR122-silenced cells that stably overexpressed SOCS3 (Fig. 5c). These results suggest that the enhanced ISRE activity in miR122-silenced cells is

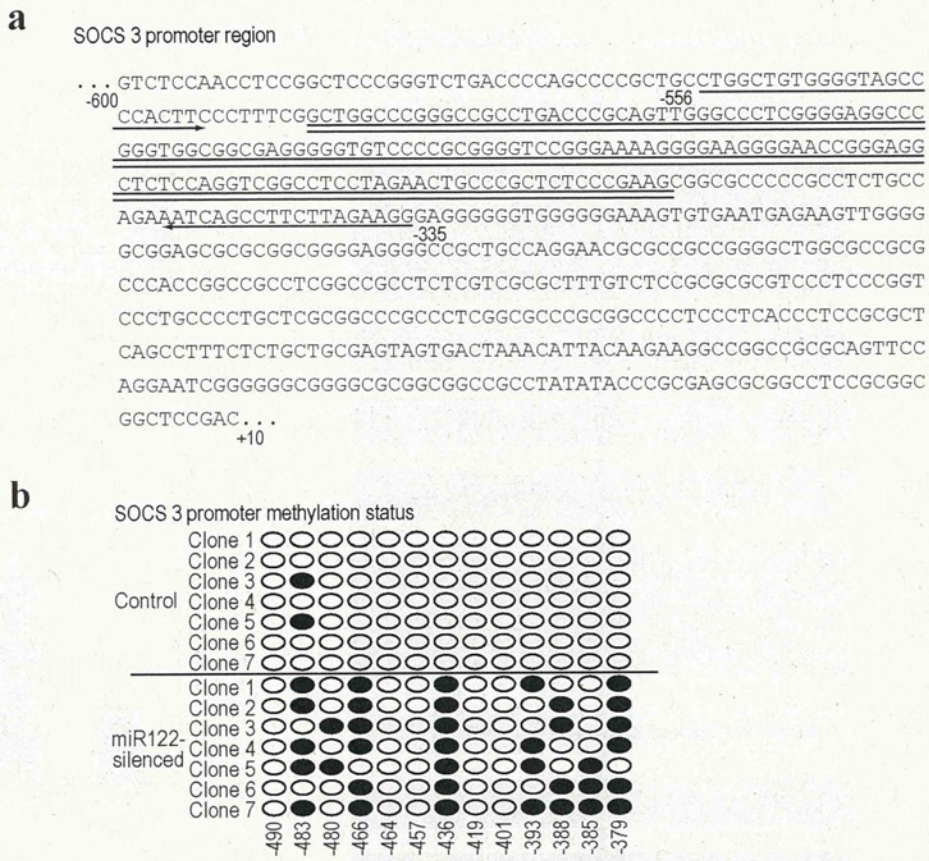


**Figure 3 | CpG methylation status in the SOCS3 promoter.** (a) The CpG island in the SOCS3 promoter is indicated by double underlines. The numbers are the positions relative to the transcription start site. Primers used for the bisulphate sequences in this study are indicated by arrows. (b) Methylation status in the CpG island of the SOCS3 promoter in control and miR122-silenced Huh7 cells, determined by the bisulphate sequences. Seven clones each were sequenced. Circles represent CpG sites. Black circles, methylated CpG sites.

mostly, if not completely, dependent on the reduced expression of SOCS3.

**MiR122 silencing enhances ISGF3-DNA binding.** Type I IFNs (IFN-α and -β) activate STATs by phosphorylation, followed by formation of the ISGF3 complex, which is composed of STAT1, STAT2, and IRF9. The importance of ISGF3 in antiviral responses is well established[29]. In contrast, the precise role of STAT3 in type I IFN signaling is not completely understood[30]. However, numerous clinicopathological results suggest that increased SOCS3 expression in the liver is closely related to a poor response to IFN therapy for HCV eradication[8,9]. This in turn suggests that high SOCS3 expression and low STAT3 activation may be related to impaired ISGF3 complex activation. In addition, STAT3 activation supports the ISGF3-dependent induction of antiviral genes *in vitro*[31]. Based on these reports, and because SOCS3 expression was lower in miR122-silenced cells (Fig. 4), we hypothesized that the level of ISGF3 complex after IFN-α treatment is higher in miR122-silenced cells, leading to greater ISRE activation (Fig. 2). While the levels of Oct-1-DNA binding as a loading control were not changed, activation of ISGF3 binding to an ISRE-containing oligonucleotide after IFN-α treatment was significantly greater in miR122-silenced cells (Fig. 6a, b, c), consistent with the fact that ISRE activities were enhanced in miR122-silenced cells in a reporter assay (Fig. 2). These data suggest that miR122-silencing in hepatocytes results in low SOCS3 expression via promoter methylation, which may subsequently enhance the induction of IFN-stimulated gene expression by increasing ISGF3-ISRE binding activities triggered by type I IFN treatment.

## Discussion

Although the treatment options for HCV infection are changing due to the introduction of HCV protease inhibitors and DAAs, the principal drug for HCV therapy remains IFN. In this study, we demonstrated that the reduced expression of miR122 contributes to decreased SOCS3 expression via promoter methylation and, subsequently, enhanced ISRE activity results after IFN-α stimulation. These data provide a molecular rationale for, and a method for increasing the efficacy of, IFN therapy for HCV infection.

MicroRNAs are involved in various biologically important intracellular signaling pathways[15–18]. Regarding the convergence of microRNAs and IFN signaling, some microRNAs are reported to be involved in endogenous IFN production in the innate immune response induced by pathogen infection[32]. In addition, several microRNAs that may regulate genes that have anti-pathogen effects are induced by IFN stimulation[33]. In this study, however, the level of miR122 expression seemed to determine the efficacy of the signaling triggered by the exogenous IFN used as an anti-HCV therapy.

MiR122 is the most abundant microRNA in the liver[24], where it has many important biological roles, such as in fatty acid metabolism[26,34] and circadian rhythms[35] under normal conditions. Further, it is also a determinant of the biological aggressiveness of hepatocellular carcinoma[36] in the pathological state. In general, microRNAs act as repressors of target gene expression[37]. However, regarding miR122 and HCV, miR122 somehow enhanced HCV RNA replication in an *in vitro* replicon system[38]. Although the precise molecular mechanisms underlying this phenomenon remain unknown, antisense miR122 has been developed as a therapeutic drug for HCV based

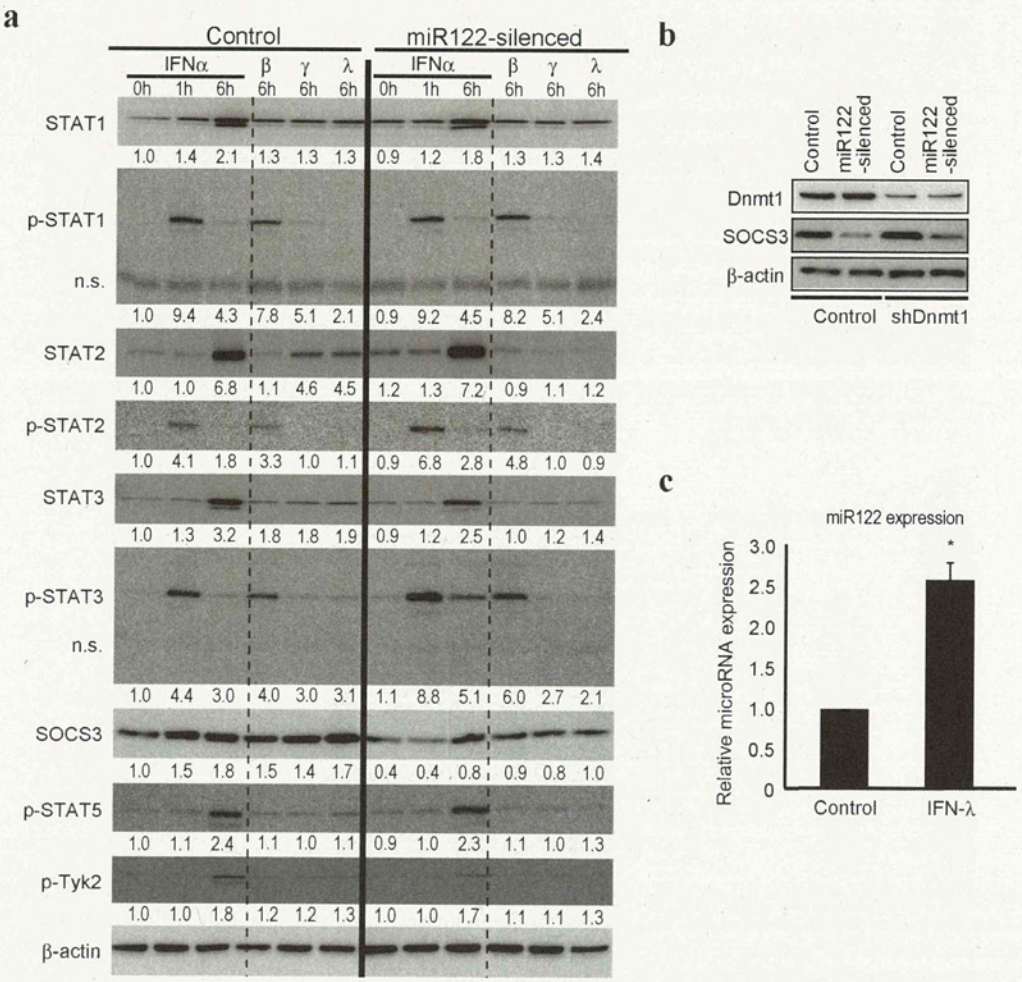


**Figure 4 | SOCS3 expression is decreased by miR122 silencing.** (a) Protein levels of the indicated IFN signaling-related genes were determined using control and miR122-silenced Huh7 cells after IFN-α, β, γ, or λ stimulation at the indicated time points. A representative of three independent determinations is shown. n.s. indicates non-specific bands. The band intensities were quantitated and adjusted by the expression levels of β-actin. The calculated ratios are indicated below each panel after setting the value of control cells at 0 h as 1.0. (b) Dnmt1 was not involved in the SOCS3 promoter methylation induced by miR122 silencing. SOCS3 protein levels were determined using control, miR122-silenced, Dnmt1 knocked-down, and Dnmt1 knocked-down with miR122-silenced Huh7 cell lysates. A representative of three independent determinations is shown. (c) MiR122 expression levels after IFN-λ stimulation for 6 h in Huh7 cells were determined by quantitative RT-PCR. Results were calculated by normalizing to U6 amounts and the relative ratio was determined by setting the value of unstimulated cells as 1. Data represent the mean ± SD of three independent determinations. *, $p < 0.05$.

on *in vitro* data[39]. Indeed, treatment of chronically HCV-infected chimpanzees with a locked nucleic acid (LNA)-modified oligonucleotide (SPC3649) complementary to miR122 leads to long-lasting suppression of HCV viremia[39]. Development of this drug for human use is now in Phase IIa trials[40]. Because our results showed that lower expression of miR122 leads to augmentation of the intracellular signaling induced by IFN, a combination therapy consisting of an antisense of miR122 and type I IFNs represents a promising and realistic therapeutic option. In addition, because IFN-α/β was reported to suppress miR122 expression, which is considered one of the mechanisms of action of IFN against HCV[41], the effects of exogenous IFN may be self-augmented by the decreased expression of SOCS3 due to decreased miR122 expression. High expression levels of SOCS3 in the liver are negative predictors of IFN treatment of HCV infection[8,9]. This may reflect suppression of IFN signaling by the high miR122 levels in the liver, as suggested by our data.

Our results indicate that reduced miR122 function leads to promoter methylation and decreased SOCS3 expression, which is possibly not the direct target of miR122, because no predictable sites for miR122 interaction in its 3′UTR were found in a computational search. A hypothesis involving an epigenetics-microRNA regulatory circuit has emerged recently[20]. While a number of microRNAs are regulated epigenetically, others simultaneously regulate epigenetic pathway-related molecules. Taken together, these results suggest that post-transcriptional regulation by microRNAs and transcriptional control machinery by epigenetics cooperate to determine the global gene expression profile and to maintain physiological functions in cells[20]. In our genome-wide study, methylation levels of a subset of gene CpG islands were aberrantly induced by miR122 silencing. While our data suggest that SOCS3 methylation was not mediated by Dnmt1, the precise mechanisms of the aberrant methylation induced by miR122, including whether it operates through regulation of the expression of other genes or directly in the nucleus, remains to be elucidated. Nonetheless, our results indicate that aberrant functions of some miRNAs may lead to changes in the methylation levels of a subset of gene CpG islands.

Recent genome-wide association studies have discovered a significant association between the response to pegIFN and ribavirin

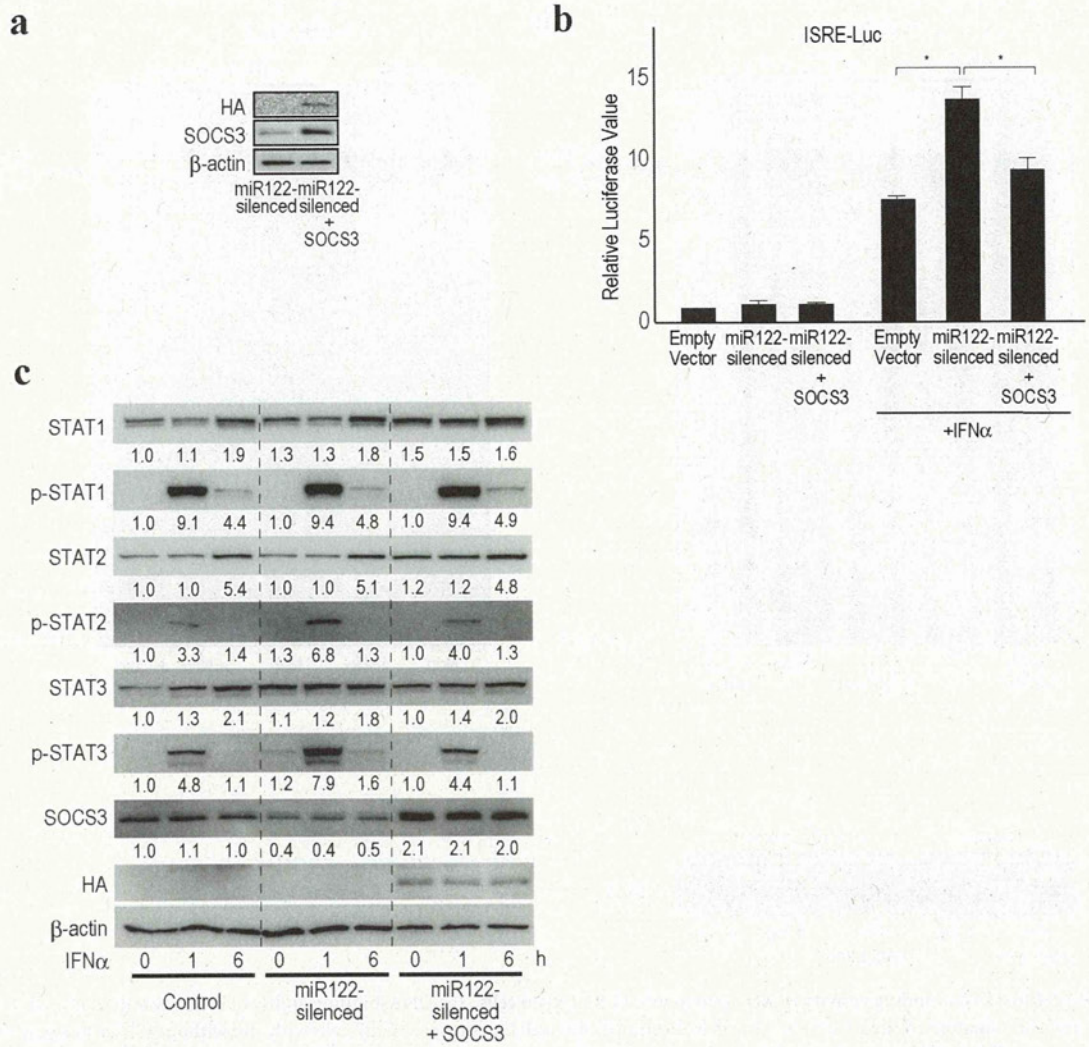


**Figure 5 | SOCS3 overexpression in miR122-silenced Huh7 cells reverses enhanced ISRE activities.** (a) HA-tagged SOCS3 was overexpressed in miR122-silenced Huh7 cells. Representative blotting images are shown. (b) SOCS3 overexpression suppresses enhanced ISRE activities in miR122-silenced Huh7 cells by a reporter assay. *, $p < 0.05$. Data represent the means ± SD of three independent determinations. (c) SOCS3 overexpression restored STAT2 and STAT3 phosphorylation levels induced by IFN-α in miR122-sileced Huh7 cells. A representative of three independent determinations is shown. The band intensities were quantitated and adjusted by the expression levels of β-actin. The calculated ratios are indicated below each panel after setting the value of control cells at 0 h as 1.0.

therapy and common single nucleotide polymorphisms in the vicinity of IL-28 (IFN-λ) genes[42,43]. In addition, carriers of the alleles associated with resolution of HCV infection have increased serum IFN-λ levels[43]. Our results demonstrate that IFN-λ stimulation increases SOCS3 and miR122 expression, which may block innate type I IFN signaling. This seems inconsistent with the fact that patients with high IFN-λ levels have better responses to pegIFN and ribavirin therapy. However, we speculate that blockade of innate IFN-α signaling by high IFN-λ through SOCS3 expression may prevent the chronically low levels of innate IFN-α, which may increase the sensitivity to exogenous IFN-α when applied in therapeutic quantities. Although further work is required, it is consistent with the fact that low expression of hepatic IFN-stimulated genes (ISGs) is strongly associated with a better response to IFN treatment and genetic variation in IL-28B[44,45].

Higher expression of α-fetoprotein (AFP) is also known as a poor prognostic factor for IFN treatment in HCV therapy[46,47]. As we described previously, decreased expression levels of miR122 are linked to increased expression of AFP[36]. Therefore, in cases with higher AFP levels, miR122 levels in hepatocytes may be low and thus, innate IFN signaling may be high through SOCS3 promoter methylation. These may provide a molecular explanation of the poor response to IFN therapy in cases with high AFP levels.

In summary, our study provides information on the involvement of miR122 in the regulation of ISRE activity through the modulation of SOCS3 expression via gene promoter methylation. Our results provide a molecular rationale that will facilitate more effective use of IFN as an anti-HCV combination therapy, specifically by including modulators of miR122 function.

## Methods

**Cell culture.** The human hepatocellular carcinoma cell lines Huh7 and HepG2 were obtained from the Japanese Collection of Research Bioresources (JCRB, Osaka, Japan). The human embryonic kidney cell line 293T was obtained from the American Type Culture Collection (ATCC, Rockville, MD). MiR122 functionally knocked-down Huh7 (miR122-silenced Huh7) cell lines were as described previously[36]. Hela-Tet-Off cell lines were purchased from Clontech (Mountain View, CA). Huh7-Tet-Off cell lines were established by transfecting with the pTet-Off vector (Clontech) and selecting with 400 μg/ml G418 (Wako, Osaka, Japan). All cells were maintained in Dulbecco's modified Eagle's medium, supplemented with 10% fetal bovine serum.

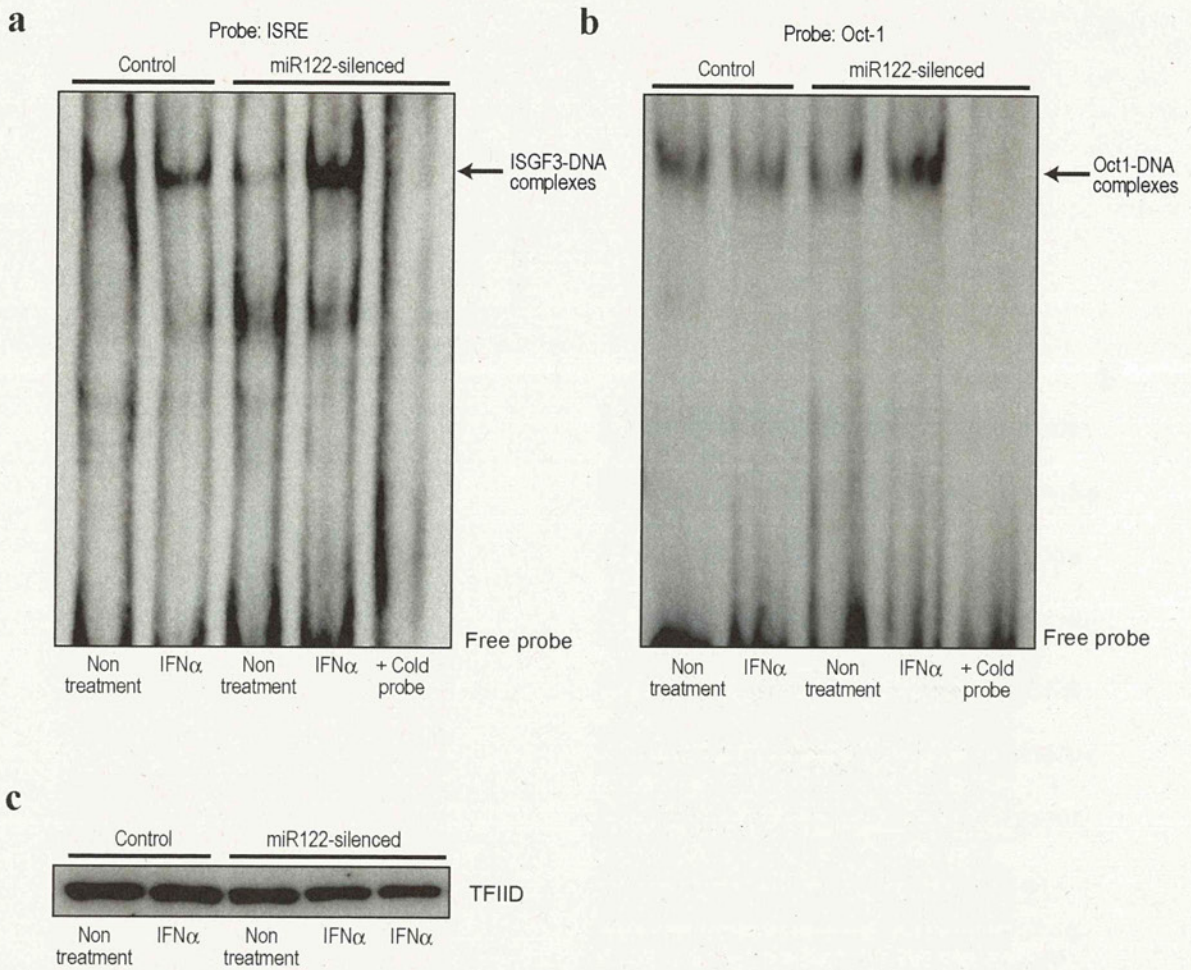


**Figure 6 | ISGF3-ISRE DNA binding activity is increased in miR122-silenced cells.** (a) DNA-binding ability of ISGF3 was determined by gel shift assay using ISRE consensus oligonucleotides. Nuclear extracts from control and miR122-silenced Huh7 cells with and without IFN-α stimulation for 1 h were used. Arrow indicates ISGF3-DNA complexes. The specificity of the DNA–protein complex was tested by adding unlabeled ISRE probe (cold probe) to IFN-α-stimulated miR122-silenced Huh7 nuclear extracts. A representative of three independent determinations is shown. (b) DNA-binding ability of Oct-1 was determined as a control for equal loading of nuclear extract. (c) TFIID amounts were examined by Western blotting to confirm equal nuclear extract loading. A representative of two independent determinations is shown.

**Reagents.** Human recombinant IFN-α, IFN-β, IFN-γ, and IL-28B (IFN-λ3) were purchased from R&D Systems (Minneapolis, MN) and used at final concentrations of 100 U/ml, 100 U/ml, 10 ng/mL, and 100 ng/mL, respectively. Doxycyclin and Tet-system fetal bovine serum were purchased from Clontech. Hygromycin was purchased from EMD Chemicals (Darmstadt, Germany).

**Stable reporter cell lines and microRNA screening.** To establish ISRE-luc reporter cell lines, 293T cells were transfected with the reporter plasmid pISRE-luc (Clontech) with a linear hygromycin resistance marker (Clontech). Single clones were selected in the presence of 250 μg/mL hygromycin. To screen for microRNAs that modulate ISRE activity, 75 microRNAs that are highly expressed in the liver[34], were reverse-transfected as described previously[15]. Briefly, synthetic mature microRNAs and, as a negative control, double-stranded RNA with artificial sequences (B-Bridge, Sapporo, Japan) were applied, with transfection reagents, to 96-well plates. The reporter cells were seeded to the plates, reverse-transfected, and then incubated for 48 h. ISRE-derived luciferase activity was measured using a GloMax 96 Microplate Luminometer (Promega, Madison, WI) after exposure to IFN-α for 12 h. Determinations were performed in duplicate, and the data were compared to those of the negative control.

**Plasmids and tetracycline-inducible stable cell lines.** The miR122 precursor expression plasmid was described previously[36]. The miR885 precursor expression plasmid was constructed by inserting a polymerase chain reaction (PCR)-generated 500 bp sequence encoding the miR885 precursor into the pCDH vector (System Biosciences, Mountain View, CA) using the *XbaI* and *NotI* sites. The resulting plasmid drives expression of miR885 under control of the CMV promoter. Plasmids expressing Halo-tagged SOCS3 were purchased from Promega. HA-tagged SOCS3 cDNA was amplified by PCR using the Halo-tagged SOCS3 plasmid as a template and the product was cloned into the pCDH-neo vector (System Biosciences) at the *NotI* site using In-fusion cloning method (Clontech). Plasmids expressing p53 were described previously[48]. To construct a tetracycline-regulated miR122 precursor expression plasmid, a PCR-amplified 500 bp region encoding themiR122 precursor was inserted into the pTRE2 vector (Clontech) using the *BamHI* and *SalI* sites. To establish tetracycline-regulated miR122 expressing stable cell lines, pTRE2miR122 plasmids were transfected into Hela-Tet-Off or Huh7-Tet-Off cell lines with a linear hygromycin marker (Clontech), followed by selection with hygromycin. Cells were cultured with or without 2.5 μg/ml doxycyclin. To establish SOCS3 overexpressing stable cells, HA-tagged SOCS3 expressing lentiviral particles were produced as described previously[36] and transduced into miR122-silenced Huh7 cells, followed by selection with G418 (Sigma, St. Louis, MO).

**Lentiviral transduction.** Huh7 cells were transduced with Dnmt1-shRNA and control-shRNA lentiviral particles (Santa Cruz Biotechnology, Santa Cruz, CA) and then selected on puromycin.

**Western blot analysis and antibodies.** Western blotting was performed as described previously[49]. All antibodies were purchased from Cell Signaling Technology (Danvers, MA), except anti-HA (Roche Applied Science, Indianapolis, IN) and anti-β-actin (Sigma).

**Transfection and luciferase assay.** Plasmid transfection was performed using FuGENE6 (Boehringer Mannheim, Mannheim, Germany) according to the manufacturer's protocol[36]. Luciferase activities were measured using a Dual Luciferase Reporter Assay System (Promega) as described previously[50].

**Genome-wide DNA methylation analysis.** Comprehensive DNA methylation analyses were performed by the outsourcing company MBL (Nagoya, Japan) using the Illumina Infinium methylation assay (Human Methylation27 BeadChip), which provides quantitative methylation levels at 27,578 promoter-associated CpG sites. Genomic DNA extracted from control and miR122-silenced Huh7 cells using QIAamp DNA mini kit (QIAGEN, Hilden, Germany) was used for this assay. Promoters with differential methylation levels were determined based on the standard criteria that differential values above 0.15 indicate significant differences in methylation status[51].

**Bisulphite sequence analyses.** Bisulphite sequence analyses were performed to check the methylation status of the SOCS3 promoter. Genomic DNA was extracted by QIAamp DNA mini kit (Qiagen) and bisulphate modified using MethylEasy Xceed Bisulphite Modification Kit (Human Genetic Signatures, North Ryde, Australia). The sequences of the SOCS3 promoter region were extracted as the upstream sequence of the transcriptional start site. The region of CpG islands and the PCR primers were determined using the web-based software MethPrimer[52]. PCR was performed using EpiTaq HS enzyme (TaKaRa, Shiga, Japan), according to the manufacturer's instructions. The PCR products were gel-purified using the QIAquick Gel Extraction Kit (Qiagen) and cloned into the TA vector using TOPO-TA cloning (Invitrogen). Seven clones from each sample were selected and the sequences were analyzed using a 3700 DNA analyzer (Applied Biosystems, Foster City, CA). The results were summarized using the web-based software, QUMA (http://quma.cdb.riken.jp/top/quma_main_j.html).

**RNA extraction and quantitative RT-PCR analysis of microRNA expression levels.** Total RNA was isolated from cells using Trizol Reagent (Invitrogen, Carlsbad, CA). To determine the levels of miR122 expression, cDNA was synthesized from RNA, and quantitative PCR was performed using an Mir-X miRNA First-Strand Synthesis and SYBR qRT-PCR Kit (Clontech). Relative expression values of microRNAs were calculated by the *CT*-based calibrated standard curve method. These values were then normalized to that of the U6 snRNA.

**Electrophoretic mobility shift assay (EMSA).** Nuclear extracts were prepared as described previously[53]. Five micrograms of nuclear extract were incubated with a double-stranded biotin-labeled DNA probe containing ISRE sites (5′-GAT CCA TGC CTC GGG AAA GGG AAA CCG AAA CTG AAG CC-3′)[54] or Oct-1 sites (Affymetrix, Santa Clara, CA) plus 1-μg poly (dI-dC) in a binding buffer (50 mM Tris [pH 7.5], 250 mM NaCl, 2.5 mM DTT, 2.5 mM EDTA, 5 mM $MgCl_2$, and 20% glycerol) at 15°C for 30 min. DNA–protein complexes were separated on 6% non-denaturing polyacrylamide gels in 0.5× TBE (25 mM Tris base, 24.25 mM boric acid, and 1 mM disodium EDTA) by electrophoresis at 120 V, 4°C for 30 min, and then transferred to Presoak Pall Biodyne B nylon membranes (Hybond-N$^+$; GE Healthcare Life Sciences) by electrophoresis in the same buffer for 30 min at 300 mA. Oligonucleotides were fixed using a UV cross-linker, and visualized using the LightShift Chemiluminescent EMSA Kit (Thermo Scientific, Rockford, IL), according to the manufacturers' instructions.

**Statistical analysis.** Statistically significant differences between groups were determined using Student's *t*-test when variances were equal. When variances were unequal, Welch's *t*-test was used. *P*-values less than 0.05 were considered statistically significant.


1. Hofmann, W. P. & Zeuzem, S. A new standard of care for the treatment of chronic HCV infection. *Nat Rev Gastroenterol Hepatol* **8**, 257–264 (2011).
2. Di Bisceglie, A. M. *et al.* Prolonged therapy of advanced chronic hepatitis C with low-dose peginterferon. *N Engl J Med* **359**, 2429–2441 (2008).
3. Hoofnagle, J. H. A step forward in therapy for hepatitis C. *N Engl J Med* **360**, 1899–1901 (2009).
4. Stetson, D. B. & Medzhitov, R. Type I interferons in host defense. *Immunity* **25**, 373–381 (2006).
5. Schindler, C. Teaching resources. Cytokine receptors and Jak-STAT signaling. *Sci STKE* **2006,** (2006).
6. Yoshimura, A., Naka, T. & Kubo, M. SOCS proteins, cytokine signalling and immune regulation. *Nat Rev Immunol* **7**, 454–465 (2007).
7. Funaoka, Y. *et al.* Analysis of interferon signaling by infectious hepatitis C virus clones with substitutions of core amino acids 70 and 91. *J Virol* **85**, 5986–5994 (2011).
8. Kim, K. A. *et al.* Hepatic SOCS3 expression is strongly associated with non-response to therapy and race in HCV and HCV/HIV infection. *J Hepatol* **50**, 705–711 (2009).
9. Miyaaki, H. *et al.* Predictive value of suppressor of cytokine signal 3 (SOCS3) in the outcome of interferon therapy in chronic hepatitis C. *Hepatol Res* **39**, 850–855 (2009).
10. Shao, R. X. *et al.* Suppressor of cytokine signaling 3 suppresses hepatitis C virus replication in an mTOR-dependent manner. *J Virol* **84**, 6060–6069 (2010).
11. Carrington, J. & Ambros, V. Role of microRNAs in plant and animal development. *Science* **301**, 336–338 (2003).
12. Bartel, D. P. MicroRNAs: genomics, biogenesis, mechanism, and function. *Cell.* **116**, 281–297 (2004).
13. Ambros, V. The functions of animal microRNAs. *Nature* **431**, 350–355 (2004).
14. Lu, J. *et al.* MicroRNA expression profiles classify human cancers. *Nature* **435**, 834–838 (2005).
15. Takata, A. *et al.* MicroRNA-22 and microRNA-140 suppress NF-κB activity by regulating the expression of NF-κB coactivators. *Biochem Biophys Res Commun* **411**, 826–831 (2011).
16. Park, S. Y., Lee, J. H., Ha, M., Nam, J. W. & Kim, V. N. miR-29 miRNAs activate p53 by targeting p85 alpha and CDC42. *Nat Struct Mol Biol* **16**, 23–29 (2009).
17. Kasinski, A. L. & Slack, F. J. Potential microRNA therapies targeting Ras, NFkappaB and p53 signaling. *Curr Opin Mol Ther* **12**, 147–157 (2010).
18. Ma, X., Becker Buscaglia, L. E., Barker, J. R. & Li, Y. MicroRNAs in NF-{kappa}B signaling. *J Mol Cell Biol* **3**, 159–166 (2011).
19. Hwang, H. W., Wentzel, E. A. & Mendell, J. T. A hexanucleotide element directs microRNA nuclear import. *Science* **315**, 97–100 (2007).
20. Wu, L. *et al.* DNA methylation mediated by a microRNA pathway. *Mol Cell* **38**, 465–47 (2010).
21. Sato, F., Tsuchiya, S., Meltzer, S. J. & Shimizu, K. MicroRNAs and epigenetics. *FEBS J* **278**, 1598–1609 (2011).
22. Fabbri, M. & Calin, G. A. Epigenetics and miRNAs in human cancer. *Adv Genet* **70**, 87–99 (2010).
23. Saetrom, P., Snøve, O. & Rossi, J. J. Epigenetics and microRNAs. *Pediatr Res* **61**, 17R–23R (2007).
24. Landgraf, P. *et al.* A mammalian microRNA expression atlas based on small RNA library sequencing. *Cell* **129**, 1401–1414 (2007).
25. Bhattacharyya, S., Habermacher, R., Martine, U., Closs, E. & Filipowicz, W. Relief of microRNA-mediated translational repression in human cells subjected to stress. *Cell* **125**, 1111–1124 (2006).
26. Esau, C. *et al.* miR-122 regulation of lipid metabolism revealed by in vivo antisense targeting. *Cell Metab* **3**, 87–98 (2006).
27. Li, E., Beard, C. & Jaenisch, R. Role for DNA methylation in genomic imprinting. *Nature* **366**, 362–365 (1993).
28. Brierley, M. M. & Fish, E. N. Stats: multifaceted regulators of transcription. *J Interferon Cytokine Res* **25**, 733–744 (2005).
29. Platanias, L. C. Mechanisms of type-I- and type-II-interferon-mediated signalling. *Nat Rev Immunol* **5**, 375–386 (2005).
30. Icardi, L. *et al.* Opposed regulation of type I IFN-induced STAT3 and ISGF3 transcriptional activities by histone deacetylases (HDACS) 1 and 2. *FASEB J* **26**, 240–9 (2011).
31. Ho, H. H. & Ivashkiv, L. B. Role of STAT3 in type I interferon responses. Negative regulation of STAT1-dependent inflammatory gene activation. *J Biol Chem* **281**, 14111–14118 (2006).
32. Gantier, M. P. New perspectives in MicroRNA regulation of innate immunity. *J Interferon Cytokine Res* **30**, 283–289 (2010).
33. David, M. Interferons and microRNAs. *J Interferon Cytokine Res* **30**, 825–828 (2010).
34. Krützfeldt, J. *et al.* Silencing of microRNAs in vivo with 'antagomirs'. *Nature* **438**, 685–689 (2005).
35. Gatfield, D. *et al.* Integration of microRNA miR-122 in hepatic circadian gene expression. *Genes Dev* **23**, 1313–1326 (2009).
36. Kojima, K. *et al.* MicroRNA122 is a key regulator of α-fetoprotein expression and influences the aggressiveness of hepatocellular carcinoma. *Nat Commun* **2**, 338 (2011).
37. Bartel, D. P. MicroRNAs: target recognition and regulatory functions. *Cell* **136**, 215–233 (2009).
38. Jopling, C., Yi, M., Lancaster, A., Lemon, S. & Sarnow, P. Modulation of hepatitis C virus RNA abundance by a liver-specific MicroRNA. *Science* **309,** (2005).
39. Lanford, R. E. *et al.* Therapeutic silencing of microRNA-122 in primates with chronic hepatitis C virus infection. *Science* **327**, 198–201 (2010).
40. Sheridan, C. New Merck and Vertex drugs raise standard of care in hepatitis C. *Nat Biotechnol* **29**, 553–554 (2011).
41. Pedersen, I. M. *et al.* Interferon modulation of cellular microRNAs as an antiviral mechanism. *Nature* **449**, 919–922 (2007).
42. Suppiah, V. *et al.* IL28B is associated with response to chronic hepatitis C interferon-alpha and ribavirin therapy. *Nat Genet* **41**, 1100–1104 (2009).
43. Tanaka, Y. *et al.* Genome-wide association of IL28B with response to pegylated interferon-alpha and ribavirin therapy for chronic hepatitis C. *Nat Genet* **41**, 1105–1109 (2009).
44. Pillai, R. S., Bhattacharyya, S. N. & Filipowicz, W. Repression of protein synthesis by miRNAs: how many mechanisms? *Trends Cell Biol.* **17**, 118–126 (2007).
45. Honda, M. *et al.* Hepatic ISG expression is associated with genetic variation in interleukin 28B and the outcome of IFN therapy for chronic hepatitis C. *Gastroenterology* **139**, 499–509 (2010).
46. Akuta, N. *et al.* Predictors of viral kinetics to peginterferon plus ribavirin combination therapy in Japanese patients infected with hepatitis C virus genotype 1b. *J Med Virol* **79**, 1686–1695 (2007).
47. Akuta, N. *et al.* Substitution of amino acid 70 in the hepatitis C virus core region of genotype 1b is an important predictor of elevated alpha-fetoprotein in patients without hepatocellular carcinoma. *J Med Virol* **80**, 1354–1362 (2008).
48. Dharel, N. *et al.* Potential contribution of tumor suppressor p53 in the host defense against hepatitis C virus. *Hepatology* **47**, 1136–1149 (2008).
49. Otsuka, M. *et al.* Hypersusceptibility to vesicular stomatitis virus infection in Dicer1-deficient mice is due to impaired miR24 and miR93 expression. *Immunity* **27**, 123–134 (2007).
50. Otsuka, M. *et al.* Impaired microRNA processing causes corpus luteum insufficiency and infertility in mice. *J Clin Invest* **118**, 1944–1954 (2008).

51. Bibikova, M. *et al.* Genome-wide DNA methylation profiling using Infinium assay. *Epigenomics* **1**, 177–200 (2009).
52. Li, L. C. & Dahiya, R. MethPrimer: designing primers for methylation PCRs. *Bioinformatics* **18**, 1427–1431 (2002).
53. Schreiber, E., Matthias, P., Müller, M. & Schaffner, W. Rapid detection of octamer binding proteins with 'mini-extracts', prepared from a small number of cells. *Nucleic Acids Res* **17**, 6419 (1989).
54. Wong, L. H., Hatzinisiriou, I., Devenish, R. J. & Ralph, S. J. IFN-gamma priming up-regulates IFN-stimulated gene factor 3 (ISGF3) components, augmenting responsiveness of IFN-resistant melanoma cells to type I IFNs. *J Immunol* **160**, 5475–5484 (1998).

## Acknowledgments

This work was supported by Grants-in-Aid from the Ministry of Education, Culture, Sports, Science and Technology, Japan (#22390058, #24590956 and #20390204) (to M.O., H.Y. and K.Koike), by Health Sciences Research Grants of The Ministry of Health, Labour and Welfare of Japan (Research on Hepatitis) (to K.Koike) and grants from the Mochida Memorial Foundation for Medical and Pharmaceutical Research, the Yakult Bio-Science Foundation and the Cell Science Research Foundation (to M.O.).

## Author contributions

T.Y., A.T., and M.O. planned the research and wrote the paper. T.Y., A.T., M.O., and T.K. performed the experiments. H.Y. analyzed the data. K.K. supervised the entire project.

## Additional information

**Competing financial interests:** The authors declare no competing financial interests.



**How to cite this article:** Yoshikawa, T. *et al.* Silencing of microRNA-122 enhances interferon-α signaling in the liver through regulating SOCS3 promoter methylation. *Sci. Rep.* **2**, 637; DOI:10.1038/srep00637 (2012).

J Gastroenterol (2012) 47:187–194
DOI 10.1007/s00535-011-0477-8

ORIGINAL ARTICLE—LIVER, PANCREAS, AND BILIARY TRACT

# Serum gamma-glutamyltransferase level is associated with serum superoxide dismutase activity and metabolic syndrome in a Japanese population

**Hayato Nakagawa · Akihiro Isogawa · Ryosuke Tateishi · Mizuki Tani · Haruhiko Yoshida · Minoru Yamakado · Kazuhiko Koike**

Received: 27 June 2011 / Accepted: 16 August 2011 / Published online: 6 October 2011


**Abstract**
*Background* Serum gamma-glutamyltransferase level has attracted considerable attention as a predictor of various conditions, such as cardiovascular disease and cancer. Although the mechanism that links the serum gamma-glutamyltransferase level to these diseases is not fully understood, one explanation is that gamma-glutamyltransferase may be closely related to oxidative stress. We conducted a large cross-sectional study to evaluate the relationship between serum gamma-glutamyltransferase and oxidative stress.
*Methods* We examined anti-oxidative stress activity and accumulation of oxidative stress in serum obtained from 2907 subjects who underwent a complete health check-up. We used serum total superoxide dismutase activity as an index of anti-oxidative stress activity. Superoxide dismutase is one of the most important intracellular and extracellular defense systems against superoxide, but the relationship between serum superoxide dismutase activity and the serum gamma-glutamyltransferase level is unclear.
*Results* The serum gamma-glutamyltransferase level was negatively correlated with serum superoxide dismutase activity, a correlation that was observed even within the normal range. A subgroup analysis stratified by the amount of alcohol consumed also showed a similar correlation. In contrast, the serum gamma-glutamyltransferase level was positively correlated with serum lipid peroxide level, even in the normal range. Furthermore, an increased serum gamma-glutamyltransferase level was significantly associated with the progression of metabolic syndrome and carotid artery intima-media thickness.
*Conclusions* The serum gamma-glutamyltransferase level, even in the normal range, was significantly associated with anti-oxidative stress activity, the accumulation of oxidative stress, metabolic syndrome, and atherosclerosis. Measuring the serum gamma-glutamyltransferase level is simple and inexpensive, and this level can be used as a sensitive marker of oxidative stress and metabolic syndrome.

**Keywords** Gamma-glutamyltransferase · Superoxide dismutase · Lipid peroxide · Metabolic syndrome · Atherosclerosis

**Abbreviations**

| | |
|---|---|
| ALT | Alanine aminotransferase |
| BMI | Body mass index |
| CuZn-SOD | Copper/zinc-containing superoxide dismutase |
| DBP | Diastolic blood pressure |
| GGT | Gamma-glutamyltransferase |
| GSH | Glutathione |
| HDL-C | High-density lipoprotein-cholesterol |
| IMT | Intima-media thickness |
| ROS | Reactive oxygen species |
| SBP | Systolic blood pressure |
| TC | Total cholesterol |
| T-SOD | Total superoxide dismutase |

H. Nakagawa (✉) · R. Tateishi · H. Yoshida · K. Koike
Department of Gastroenterology, University of Tokyo, 7-3-1 Hongo, Bunkyo-ku, Tokyo 113-8655, Japan
e-mail: n-hayato@yf7.so-net.ne.jp

H. Nakagawa · M. Tani · M. Yamakado
Center for Multiphasic Health Testing and Services, Mitsui Memorial Hospital, 1 Kanda-Izumi-cho, Chiyoda-ku, Tokyo 101-8643, Japan

A. Isogawa
Department of Internal Medicine, Mitsui Memorial Hospital, 1 Kanda-Izumi-cho, Chiyoda-ku, Tokyo 101-8643, Japan

## Introduction

The serum gamma-glutamyltransferase (GGT) level has been widely used as an indicator of liver disease and alcohol consumption [1]. GGT has attracted considerable attention as a predictor of metabolic syndrome, insulin resistance, cardiovascular disease, stroke, and cancer [2–7]. Furthermore, elevated GGT is associated with higher all-cause mortality [8, 9].

The mechanism that links the serum GGT level to various diseases and mortality is not fully understood. One explanation is that GGT may be closely related to oxidative stress [10–12]. GGT is the enzyme responsible for the extracellular catabolism of glutathione (GSH), the main thiol intracellular antioxidant agent in most cells. Because GGT plays important roles in GSH homeostasis, GGT expression increases as an adaptive response upon exposure to oxidative stress. However, paradoxically, GGT is also directly involved in the generation of reactive oxygen species (ROS) under physiological conditions, particularly in the presence of iron or other transition metals [13]. Thus, the serum GGT level may reflect not only the response to oxidative stress, but also the generation and accumulation of oxidative stress. The serum GGT level has been associated with some oxidative stress markers, such as carotenoids, tocopherols, and lipid peroxide (LPO) [14–16].

Superoxide dismutase (SOD) exists in three isoforms: cytosolic copper/zinc-containing SOD (CuZn-SOD), mitochondrial manganese-containing SOD (Mn-SOD), and extracellular SOD [17, 18]. These enzymes contain redox metals in their catalytic centers and dismutate superoxide radicals to hydrogen peroxide and oxygen. SOD is an endogenous free-radical scavenger and one of the most important intracellular and extracellular defense systems against superoxide, an oxygen-derived free radical that has been implicated in various oxidative cell injuries. The measurement of serum total SOD (T-SOD) activity reflects systemic oxidative stress status, and its level is negatively correlated with atherosclerosis [19]. However, the relationship between serum T-SOD activity and the serum GGT level is unclear.

To evaluate the usefulness of the serum GGT level as an oxidative stress marker, we conducted a large cross-sectional study in 2907 subjects who underwent a complete health check-up. We used serum T-SOD and serum LPO levels as indexes of anti-oxidative stress activity and of the accumulation of oxidative stress, respectively. Additionally, to assess the clinical relevance of the serum GGT level, we investigated the association between the serum GGT level, metabolic syndrome, and carotid atherosclerosis.

## Methods

### Subjects

Between January 2001 and December 2003, 2907 subjects who had undergone general health screening tests, including carotid ultrasonography, at the Center for Multiphasic Health Testing Services, Mitsui Memorial Hospital, were enrolled. In Japan, regular employee health check-ups are mandated by law. Thus, the majority of these subjects had no major health problem. Blood samples were taken after an overnight fast. Data on hepatitis C core antigen and hepatitis B surface antigen were available in 2877 subjects (98.9%); 23 of these 2877 subjects were positive for hepatitis C and 40 were positive for hepatitis B. Because serum GGT levels did not differ between hepatitis-positive ($48.0 \pm 45.9$ IU/L) and -negative ($49.1 \pm 57.8$ IU/L) subjects, the hepatitis-positive subjects were not excluded.

Serum T-SOD activity was routinely determined with a computerized electron spin resonance spectrometer system (JES-FR30; JEOL, Tokyo, Japan) [19]. Serum LPO level was measured using the fluorimetric assay method of Yagi [20]. Carotid artery status was examined using a high-resolution B-mode ultrasonography instrument (Sonolayer SSA270A; Toshiba, Tokyo, Japan), equipped with a 7.5-MHz transducer (PLF-703ST; Toshiba). The carotid arteries were examined bilaterally at the level of the common carotid, the bifurcation, and the internal carotid arteries from transverse and longitudinal orientations. Carotid artery intima-media thickness (IMT) was measured, using a computer-assisted method, by experienced sonographers who were unaware of the subjects' clinical and laboratory findings.

Of the 2907 subjects, 2249 (77.3%) had undergone abdominal ultrasonography. All abdominal ultrasonography was performed with an SSD-5500 system (Aloka, Wallingford, CT, USA) and a 3.5-MHz convex probe. Fatty liver was diagnosed based on a bright liver with hepatorenal echo contrast.

This study was conducted after written informed consent was received from all subjects. The study protocol conformed to the ethical guidelines of the 1975 Declaration of Helsinki and was approved by the ethics committee of Mitsui Memorial Hospital (MEC2009-30).

### Analysis

Body mass index (BMI) was calculated as the square of weight (in kg) divided by height (in meters). We defined obesity as BMI $\geq 25$ kg/m$^2$, hypertension as systolic blood pressure $\geq$130 mmHg or diastolic blood pressure

≥85 mmHg, hypertriglyceridemia as a serum triglyceride concentration of ≥150 mg/dL, low high-density lipoprotein-cholesterol (HDL-C) as HDL-C ≤40 mg/dL for men or ≤50 mg/dL for women, and hyperglycemia as a fasting blood sugar level of ≥110 mg/dL. We defined the metabolic syndrome score as the number of these metabolic syndrome markers, based on the National Cholesterol Education Program Adult Treatment Program III definition.

Serum GGT levels were classified in sextiles; cut-off points of the sextiles for serum GGT were 16, 22, 31, 45, and 77 IU/L. We described the six categories defined by these cut-off points as categories A (serum GGT level ≤16 IU/L), B (17–22 IU/L), C (23–31 IU/L), D (32–45 IU/L), E (46–77 IU/L), and F (> 77 IU/L), respectively. We used sextile classification because we reasoned that the highest GGT group should consist of only the subjects with a serum GGT level above the upper normal limit at our institute (74 IU/L). In quartile and quintile classifications, the highest cut-off point of GGT did not exceed the upper normal limit (58 and 65 IU/L, respectively).

### Statistical analyses

Data are expressed as means ± standard deviations. Correlations between variables were analyzed using Spearman's rank correlation coefficient. Stepwise multiple linear regression analysis was used to identify variables that were independently related to serum T-SOD activity. Trends in serum T-SOD activity, LPO level, metabolic score, and IMT in relation to serum GGT levels were assessed with the Jonckheere-Terpstra test. Continuous variables were compared with the unpaired Student's *t*-test (parametric) or the Mann–Whitney *U*-test (nonparametric). A *P* value of <0.05 on a two-tailed test was considered statistically significant. Data processing and analyses were performed using StatView (ver. 5.0; SAS Institute, Cary, NC, USA) and SPSS (ver. 14.0; SPSS, Chicago, IL, USA) software.

## Results

### Subjects' characteristics

The subjects' characteristic are shown in Table 1. The frequencies of hyperglycemia, hypertension, hypertriglyceridemia, low-HDL-cholesterolemia, and obesity were 14.0, 38.1, 26.0, 8.1, and 27.3%, respectively.

### Correlation between serum T-SOD activity and GGT level

To assess whether serum T-SOD activity was linked to metabolic syndrome, we investigated the correlations between serum T-SOD activity and clinical parameters associated with metabolic syndrome. Our results revealed significant correlations between serum T-SOD activity and various clinical parameters that tended to decline with the progression of metabolic syndrome, although these correlations were generally weak (Table 2). Of these parameters, serum GGT was most strongly correlated with serum T-SOD activity ($\rho = -0.16$, $P < 0.0001$). To identify variables that were independently related to serum T-SOD activity, we performed multiple linear regression analysis. Serum T-SOD activity could be predicted by serum GGT, HDL-C, alanine aminotransferase (ALT), age, fasting

**Table 1** Baseline characteristics

| Variables | $n = 2907$ |
|---|---|
| Age (years) | 55.2 ± 10.8 |
| Sex (male/female) | 1896/1017 |
| BMI (kg/m$^2$) | 23.3 ± 3.1 |
| SBP (mmHg) | 124.4 ± 19.2 |
| DBP (mmHg) | 77.7 ± 11.7 |
| TC (mg/dL) | 209 ± 34.6 |
| HDL-C (mg/dL) | 62.1 ± 16.4 |
| TG (mg/dL) | 128 ± 115.2 |
| Glucose (mg/dL) | 98.9 ± 21.3 |
| Insulin (IU/L) | 6.1 ± 3.8 |
| GGT (IU/L) | 49.2 ± 57.6 |
| ALT (IU/L) | 27.0 ± 31.1 |
| T-SOD (U/ml) | 2.9 ± 1.2 |
| LPO (nmol/ml) | 0.8 ± 0.9 |

*BMI* Body mass index, *SBP* systolic blood pressure, *DBP* diastolic blood pressure, *TC* total cholesterol, *HDL-C* high-density lipoprotein-cholesterol, *TG* triglycerides, *GGT* gamma-glutamyltransferase, *ALT* alanine aminotransferase, *T-SOD* total superoxide dismutase, *LPO* lipid peroxide

**Table 2** Correlations between serum T-SOD activity and other parameters

| Variables | Spearman's rho | *P* |
|---|---|---|
| Age | 0.086 | <0.0001 |
| BMI | −0.15 | <0.0001 |
| SBP | −0.086 | <0.0001 |
| DBP | −0.094 | <0.0001 |
| TC | 0.06 | 0.011 |
| HDL-C | 0.146 | <0.0001 |
| TG | −0.129 | <0.0001 |
| Glucose | −0.136 | <0.0001 |
| Insulin | −0.125 | <0.0001 |
| GGT | −0.16 | <0.0001 |
| ALT | −0.071 | 0.0001 |

blood sugar, and systolic blood pressure, and standardized beta coefficients showed that, of these parameters, serum GGT had the strongest influence on T-SOD activity (Table 3). From these results, we considered that the serum GGT level was an independent and important predictor of serum T-SOD activity, although the correlation was weak. Interestingly, in the ordered categorical analysis using sextiles, serum T-SOD activity declined in a stepwise fashion even within the normal range of the serum GGT level ($P < 0.0001$; Fig. 1a).

### Correlation between serum LPO and GGT level

Next, we assessed the correlation between serum GGT and the serum LPO level, which was used as a representative marker for oxidative stress accumulation. In contrast to the serum T-SOD activity, the serum LPO level increased in a stepwise fashion even within the normal range of the serum GGT level ($P < 0.0001$; Fig. 1b). Thus, the serum GGT level closely reflected both anti-oxidative stress activity and the accumulation of oxidative stress.

**Table 3** Multiple linear regression analysis using serum T-SOD activity as dependent variable

| Variables | Standardized beta | *P* |
|---|---|---|
| Age | 0.077 | <0.0001 |
| BMI | | NS |
| SBP | −0.045 | 0.023 |
| DBP | | NS |
| TC | | NS |
| HDL-C | 0.096 | <0.0001 |
| TG | | NS |
| Glucose | −0.057 | 0.003 |
| Insulin | | NS |
| GGT | −0.112 | <0.0001 |
| ALT | −0.057 | 0.003 |

*NS* Not significant

### Correlation of serum GGT level with metabolic syndrome and IMT

To assess the clinical relevance of serum GGT levels, we investigated the correlation of the serum GGT level with the metabolic score and IMT. Similar to oxidative stress, the metabolic score also increased in a stepwise fashion, even within the normal range of the serum GGT level ($P < 0.0001$; Fig. 2). Furthermore, the serum GGT level was significantly and positively correlated with IMT ($P < 0.0001$; Fig. 3). Thus, an increased serum GGT level was associated with the metabolic syndrome and atherosclerosis.

### Influence of drinking status on the relationship of the serum GGT level to serum SOD activity and metabolic syndrome

The serum GGT level is known to be influenced by the amount of alcohol consumed. To investigate the influence of drinking status on the relationship of the serum GGT level to SOD activity and the metabolic syndrome, we stratified subjects into four groups according to the amount of alcohol consumed: never ($n = 1053$), 1–30 g/day ($n = 886$), 31–60 g/day ($n = 631$), and >60 g/day ($n = 337$). As shown in Fig. 4a, the serum GGT level showed a significant positive graded association with the amount of alcohol consumed. T-SOD activity was negatively correlated with the amount of alcohol consumed and the metabolic score was positively correlated with this parameter (Fig. 4b, c). These findings suggest that drinking status may confound the relationship of the serum GGT level to T-SOD activity and the metabolic syndrome. Therefore, to rule out the influence of drinking status, we re-analyzed these relationships after stratifying the sample based on the amount of alcohol consumed. As shown in Fig. 4d, the serum GGT level showed a significant negative correlation with serum T-SOD activity in all subgroups stratified by drinking status. Furthermore, the serum GGT level showed

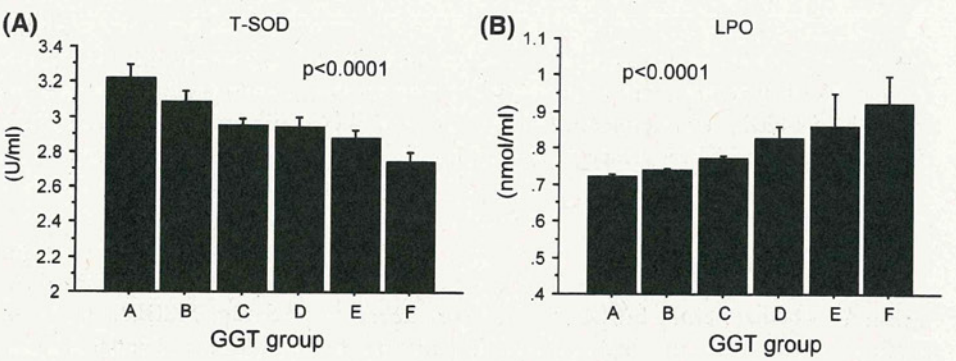


**Fig. 1** Relationship of serum gamma-glutamyltransferase (*GGT*) level to serum total superoxide dismutase (*T-SOD*) activity and lipid peroxide level. *Bar graph* shows serum T-SOD activity (**a**) and lipid peroxide (*LPO*) level (**b**) according to sextiles of serum GGT level